

**COPULA BASED RIGID-BODY IMAGE REGISTRATION**

by

**Faramarz Kashanchi**

M.Sc. Computer Science  
University of Mysore, Mysore, India.

THESIS SUBMITTED IN PARTIAL FULFILMENT OF  
THE REQUIREMENTS FOR THE DEGREE OF  
MASTER OF SCIENCE  
IN  
MATHEMATICAL, COMPUTER, AND PHYSICAL SCIENCES  
(MATHEMATICS)

UNIVERSITY OF NORTHERN BRITISH COLUMBIA

2012

© Faramarz Kashanchi, 2012



Library and Archives  
Canada

Published Heritage  
Branch

395 Wellington Street  
Ottawa ON K1A 0N4  
Canada

Bibliothèque et  
Archives Canada

Direction du  
Patrimoine de l'édition

395, rue Wellington  
Ottawa ON K1A 0N4  
Canada

*Your file Votre référence*

*ISBN: 978-0-494-94105-8*

*Our file Notre référence*

*ISBN: 978-0-494-94105-8*

#### NOTICE:

The author has granted a non-exclusive license allowing Library and Archives Canada to reproduce, publish, archive, preserve, conserve, communicate to the public by telecommunication or on the Internet, loan, distribute and sell theses worldwide, for commercial or non-commercial purposes, in microform, paper, electronic and/or any other formats.

The author retains copyright ownership and moral rights in this thesis. Neither the thesis nor substantial extracts from it may be printed or otherwise reproduced without the author's permission.

#### AVIS:

L'auteur a accordé une licence non exclusive permettant à la Bibliothèque et Archives Canada de reproduire, publier, archiver, sauvegarder, conserver, transmettre au public par télécommunication ou par l'Internet, prêter, distribuer et vendre des thèses partout dans le monde, à des fins commerciales ou autres, sur support microforme, papier, électronique et/ou autres formats.

L'auteur conserve la propriété du droit d'auteur et des droits moraux qui protègent cette thèse. Ni la thèse ni des extraits substantiels de celle-ci ne doivent être imprimés ou autrement reproduits sans son autorisation.

---

In compliance with the Canadian Privacy Act some supporting forms may have been removed from this thesis.

While these forms may be included in the document page count, their removal does not represent any loss of content from the thesis.

Conformément à la loi canadienne sur la protection de la vie privée, quelques formulaires secondaires ont été enlevés de cette thèse.

Bien que ces formulaires aient inclus dans la pagination, il n'y aura aucun contenu manquant.

Canada

# Abstract

The literature presents a wide number of algorithms in the field of image registration. However, analysis of the literature revealed that much emphasis has not been placed on copula based image registration. Thus this thesis seeks to explain the image registration problem and how it may be solved using copula based measures. Here we are aiming to combine the MATLAB `fminsearch` optimization method with copula based alignment measure, in order to monitor the performance of copula based alignment measure in image registration. Performance of four copula functions namely, Clayton, Frank, Gaussian and Marshal-Olkin are tested in image registration algorithm. A comparison is then posited of the performance of the four copula functions in image registration. These four copula measures are then compared with the well known method of image registration alignment measure, that is the joint histogram based mutual information. The accuracy and speed of the image registration algorithm was monitored on aerial and medical (MRI) images. Since we are using rigid-body transformations, the image registration algorithm is categorized as rigid body image registration.

# Contents

<b>Abstract</b>	<b>i</b>
<b>List of Figures</b>	<b>iv</b>
<b>List of Tables</b>	<b>vii</b>
<b>Acknowledgements</b>	<b>viii</b>
<b>1 Introduction</b>	<b>1</b>
1.1 Image Registration Overview . . . . .	2
1.2 Copulas in Image Processing . . . . .	5
1.3 Literature Review of Image Registration . . . . .	6
1.4 Map of Thesis . . . . .	7
<b>2 Statement of The Research and Mathematical Concepts</b>	<b>8</b>
2.1 Statement of Research . . . . .	8
2.1.1 Image Registration Algorithm . . . . .	9
2.2 Rigid-body Transformation . . . . .	10
2.3 Calculating the Alignment Measure . . . . .	12
2.3.1 Joint Histogram Based Mutual Information . . . . .	13

2.3.2	Copula Based Alignment Measure . . . . .	16
2.3.3	Examples of Copula Based Alignment Measure . . . . .	30
2.4	Optimization . . . . .	35
<b>3</b>	<b>Experiments</b>	<b>39</b>
3.1	Experimental Images . . . . .	39
3.1.1	Magnetic Resonance Imaging (MRI) . . . . .	40
3.1.2	Which Copula ? . . . . .	43
3.2	Results of Image Registration Experiments . . . . .	43
3.2.1	Joint Histogram Mutual Information . . . . .	46
3.2.2	Clayton Copula . . . . .	48
3.2.3	Frank Copula . . . . .	50
3.2.4	Marshal-Olkin Copula . . . . .	51
3.2.5	Gaussian Copula . . . . .	52
3.3	Summary of Experiments . . . . .	54
<b>4</b>	<b>Summary and Concluding Remarks</b>	<b>60</b>
	<b>Bibliography</b>	<b>63</b>
	<b>Appendix A Software Licence and Versions</b>	<b>67</b>
A.1	MATLAB . . . . .	67
A.2	Maple . . . . .	67
	<b>Appendix B Description of Images in Experiments</b>	<b>68</b>
B.1	MRI . . . . .	68
B.2	Aerial . . . . .	68

# List of Figures

1.1	Flowchart of image registration stages . . . . .	4
2.1	Flowchart of image registration stages in this thesis . . . . .	9
2.2	Right: matrix of $x$ coordinate (xcoords) Left: matrix of $y$ coordinate (ycoords) . . . . .	10
2.3	(Left: Image $A$ Right: Image $B$ ) Two gray scale images of size $3 \times 3$ and their corresponding intensity matrices below them . . . . .	14
2.4	Clayton copula cumulative distribution function . . . . .	20
2.5	Clayton copula Probability density curves for $\theta = 0.1$ (first row left), $\theta = 0.4$ (first row right) and $\theta = 0.9$ (second row) . . . . .	21
2.6	Frank copula cumulative distribution function . . . . .	22
2.7	Frank copula Probability density curves for $\theta = 0.1$ (first row left), $\theta = 0.4$ (first row right) and $\theta = 0.9$ (second row) . . . . .	24
2.8	Marshal-Olkin copula cumulative distribution function . . . . .	25
2.9	Marshal-Olkin copula Probability density curves for $\theta = 0.1$ (first row left), $\theta = 0.4$ (first row right) and $\theta = 0.9$ (second row) . . . . .	27
2.10	Gaussian copula cumulative distribution function . . . . .	28
2.11	Gaussian copula Probability density curves for $\rho = 0.1$ (first row left), $\rho = 0.4$ (first row right) and $\rho = 0.9$ (second row) . . . . .	30

2.12	Divergence measures and mutual information calculated using four copulas . . . . .	32
2.13	Left: Column matrix of Image A Right Column matrix of Image B . . .	34
2.14	Left: Reference Image Right: Test Image bottom: Registered test image using the fminsearch and joint histogram based mutual information	37
2.15	Plot of the convergence of the fminsearch in 25 iterations . . . . .	38
3.1	P1 to P8 are the reference images and TP1 to Tp8 are the testing images	41
3.2	A1 to A8 are the reference images and TA1 to TA8 are the testing images	42
3.3	First aerial image which mis-registered using the joint histogram mutual information method. (First row left: the reference image, first row right: the test image, second row left: the registered test image, second row right: the overlap of registered test image on the reference image which is mis-registered) . . . . .	48
3.4	First aerial image which registered using the Gaussian copula method. (first row left: the reference image, first row right: the test image, second row left: the registered test image, second row right: the overlap of registered test image on the reference image) . . . . .	53
3.5	PSNR values for the 8 MRI images . . . . .	54
3.6	PSNR values for the 8 Aerial images . . . . .	55
3.7	The optimization result of the Gaussian Copula for the 4th aerial image after 87 iterations . . . . .	56
3.8	The optimization result of the Gaussian Copula for the 4th MRI image after 73 iterations . . . . .	56

3.9	Registered image of the 4th aerial image.(first row left: the reference image, first row right: the test image, second row left: the registered test image, second row right: the overlap of registered test image on the reference image)	57
3.10	Registered image of the 4th MRI image.(first row left: the reference image with ROI, first row right: the test image with ROI, second row left: the registered test image with ROI, second row right: the overlap of registered test image on the reference image)	58

# List of Tables

2.1	Joint Histogram of Image $A$ and Image $B$ . . . . .	15
2.2	Values of the divergence measures and mutual information in Figure 2.4	33
3.1	Image registration results for joint histogram mutual information . . . .	46
3.2	Image registration results for Clayton Copula . . . . .	49
3.3	Image registration results for Frank Copula . . . . .	50
3.4	Image registration results for Marshal-Olkin Copula . . . . .	51
3.5	Image registration results Gaussian Copula . . . . .	52

# Acknowledgements

I am thankful to all my friends who encouraged and supported me whenever and wherever. This thesis taught me just like life, research also has ups and downs and my friends were with me in both places.

I would like to thank Dr.Edward Dobrowolski who mentored me about the mathematical ideas and Maple software operation.

Love and thanks to my family for their unconditional support. My family's kindness and love is the reason of my being.

Most importantly I thank my supervisor Dr.Pranesh Kumar who showed me the way of life in the first place. His patience, motivation and great ideas, enlightened the way of research for me.

Last but not the least I am thankful to the professors of University of Northern British Columbia and my supervisory committee , Dr.Liang Chen and Dr.Iliya Bluskov for their guidance and support.

# Chapter 1

## Introduction

In this research we attempt to examine the information theoretic and stochastic approach in the context of image alignment. Image alignment, or in other words image registration, is an ongoing research area and there are various publications on it. Excellent reviews can be found in [10] and [2]. This thesis can be considered as a continuation of research [14] on finding a simple mathematical calculation method for alignment measure in image registration. Image registration is the problem of finding the best possible geometrical transformation in order to align the moving or test image based on the fixed or reference image. In this thesis we apply a very powerful statistical function called copula function to find the best possible geometrical transformation for the tested images. Medical (MRI) and aerial images are used as the main test cases, or in other words, input to the copula based image registration approach. In this chapter we are going to talk about various types and applications of image registration, types of images used in image registration and copula functions.

## 1.1 Image Registration Overview

Image registration is known as one of the preprocessing and image restoration stages of digital image processing [11]. Inputs to the image registration algorithms are test image and reference image which are from a same scene. The test image may be obtained at different time, view, sensor or a computer generated image. In image registration we intend to align test image based on the reference image. The differences between the images of same scene such as geometrical or intensity differences may prevent the best possible alignment of test image based on reference image. The goal of image registration is to achieve the perfect alignment between images of the same scene in spite of the geometrical or intensity differences. In the following paragraphs we will demonstrate various types of image registration methodologies and the particular method used in this thesis.

In image registration the differences or variations between the images of the same scene are of two types. First, the differences that we want to preserve; for example, a tumor in a MRI image. Second, the differences that we want to correct, which may be due to multi-modal, multi-temporal, multi-view and model-image issues of image acquisition. These image acquisition issues are explained in the following [2]:

**Multi-modal:** Modality of an image, depends on the type of sensor which acquires it. In image registration we may deal with images from the same scene taken with different types of sensors which is referred to as multi-modal images. Hence due to intensity differences, the registration of multi-modal images is more difficult compared to mono-modal images which are acquired using the same sensor.

**Multi-temporal:** Two images of the same scene may be taken at different times and hence their alignment is a challenging problem in image registration field.

**Multi-view:** Images of the same scene obtained from different view points may

change the geometrical angle and add noise to the images so image registration algorithms attempt to align these images.

**Model-image:** Images of a scene and its computer generated models may need to be aligned in order to obtain their similarities and differences.

The above classification of image distortions are used in various applications such as remote sensing [3], computer vision[4] and medical imaging[5]. It is very important to decide which one of the above four differences may be corrected using the developed image registration algorithm. In this thesis we are going to simulate the multi-view test images by intentional translation and rotation of the reference images.

Image registration methods are divided into two major categories namely feature-based and area-based which are explained in the following [2]:

**Feature-based:** Also called landmark-based approach. Here the alignment of the reference image and test image is obtained by aligning the chosen landmarks. These landmarks could be surface, points or lines. Feature-based image registration algorithms are faster than the area-base image registration algorithms. Also the mentioned drawback of feature-based methods is that their accuracy depends on the accuracy of feature identification and selection.

**Area-based:** Also called content-base approach. Here the alignment is obtained based on the intensity values of the images. Here we take the whole image as the feature and hence it is not dependent on the feature identification and selection. The drawback of this method is that it is slower than the feature-based method.

There are three steps to solve any image registration problem. These three steps are alignment measure, transformation and optimization. In Figure 1.1, the diagram shows steps of image registration algorithms.

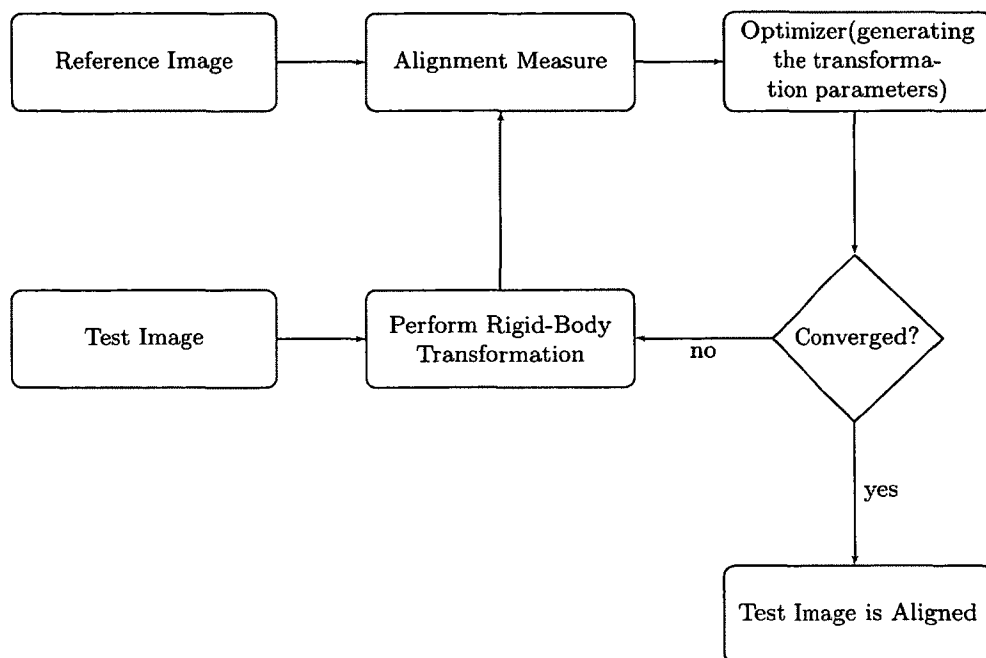


Figure 1.1: Flowchart of image registration stages

**Alignment Measure:** While matching the feature (in our thesis gray scale intensity of pixels) the alignment measure may be calculated to obtain the best alignment between the reference and test images. There are various alignment measures in the literature. Some of the popular alignment measures are the joint histogram based mutual information, divergence measure, sum of squared differences and local correlation [10].

**Transformation:** There are two types of geometrical transformations namely parametric and non-parametric transformations [2]. The instances of parametric transformation are rigid-body, affine and spline transformations. In non-parametric trans-

formation all the pixels can individually change their position. Implementation of rigid-body transformation based image registration is the target of this thesis. Rigid-body transformation consists of rotation, translation and scaling from which we make use of rotation and translation in this thesis.

**Optimization:** Image registration is also an optimization problem. Optimization is part of the image registration algorithm and it may find the most optimum transformation of the test image to align to the reference image. Some optimization algorithms are Powell's method, Downhill simplex method (fminsearch in MATLAB), gradient-descent and Levenberg-Marquardt method[23].

In summary in this thesis we are going to use the multi-view image, area-base algorithm, mutual information and divergence measure based alignment measure, rigid-body transformation and Downhill simplex optimization.

## 1.2 Copulas in Image Processing

As of our knowledge in image processing, copula functions are used in image change detection algorithms [12]. Copula function is a strong statistical tool used to represent the joint distribution in terms of the marginal distributions and dependence parameters. As obtaining the joint distribution may be a critical task, copula functions come to the rescue by generating the joint distribution by the knowledge of the marginal distributions. Unlike other joint distribution estimation methods, copula based joint distribution estimation, does not use Gaussian or Gamma distribution parameters. This is an advantage in image processing since we may not have Gaussian or Gamma distribution. Mercier uses the copula based random number generation from the two images in order to obtain a closer distribution for the best possible image change

detection between the test and reference images [13].

There are few publications on the use of copula functions in image registration. The most important publication in the field of copula based image registration is [14]. Durrani and Zeng use the Clayton copula density functions to calculate the divergence measure as the alignment measure for image registration. There are various copula families and their performance as an alignment measure in image registration can be investigated. In this thesis we are going to compare the performance of four copula functions namely, Clayton, Frank, Gaussian and Marshal- Olkin in image registration.

### 1.3 Literature Review of Image Registration

There are many publications about image registration, here we give a brief summary. In 1996 Fredrik Mess investigated the joint histogram based mutual information to estimate the rigid-body transformation in image registration. Here the performance of various interpolation and degradation and optimization functions have been analysed in mutual information based image registration [15].

In 1997 William M.Wells found that mutual information is a good measure for multi-modal image registration and it performs better than correlation and sum of squared difference base methods. He found an estimate of the transformation that registered the reference volume  $u$  and test volume  $v$  by maximizing their mutual information. Here a Parzen window based mutual information method was proposed [16].

The main inspiration for the idea in this thesis comes from TS Durrani 2001 pa-

per [14] where they applied various copula based divergence measures as alignment measure for image registration. They found that the copula based divergence measures works well in area based image registration. They used Clayton copula which is an Archimedean copula family and they did not investigate other copula families. In other paper [17], the same author, further studied the various copula based divergence measures for random numbers of normal shape and found that the copula based divergence measures behave differently on different distributions. Hence Durani stated that for various distributions we observe different behaviour of the copula based divergence measures. In the area based image registration problem we normally have images with varied distributions. Therefore we need to find, which copula based divergence measure will give us the best result in image registration.

In this thesis we are going to investigate the performance of four copula functions namely, Clayton, Frank, Gaussian and Marshal Olkin, in calculation of copula based divergence and mutual information measure. This measure is used as the alignment measure in the area based image registration. A description of the copula concepts and their families is given in [1].

## 1.4 Map of Thesis

In chapter 2, we are going to define the statement of the research and also we will present the mathematical concepts and algorithm used in this thesis. In chapter 3, we will present the experiments performed on the medical (MRI) and aerial images and we will report the pros and cons of our algorithm. In chapter 4, we will summarize the results of this thesis and provide the future work potential ahead to this research.

## Chapter 2

# Statement of The Research and Mathematical Concepts

In this chapter we are going to present the statement of research and mathematical concepts used in this thesis. After we state the research problem, we first demonstrate the overall algorithm used for image registration and then we describe rigid body transformation, alignment measures and optimization in detail.

### 2.1 Statement of Research

In this thesis we are going to combine the MATLAB `fminsearch` optimization with copula based divergence and mutual information measure and joint histogram based mutual information in order to develop an image registration algorithm. This image

registration algorithm is area based and consist of rigid body transformation. In the following we will see how the parts of the image registration algorithm are assembled.

### 2.1.1 Image Registration Algorithm

The steps used in the image registration algorithm in this thesis are as presented in Figure 2.1.

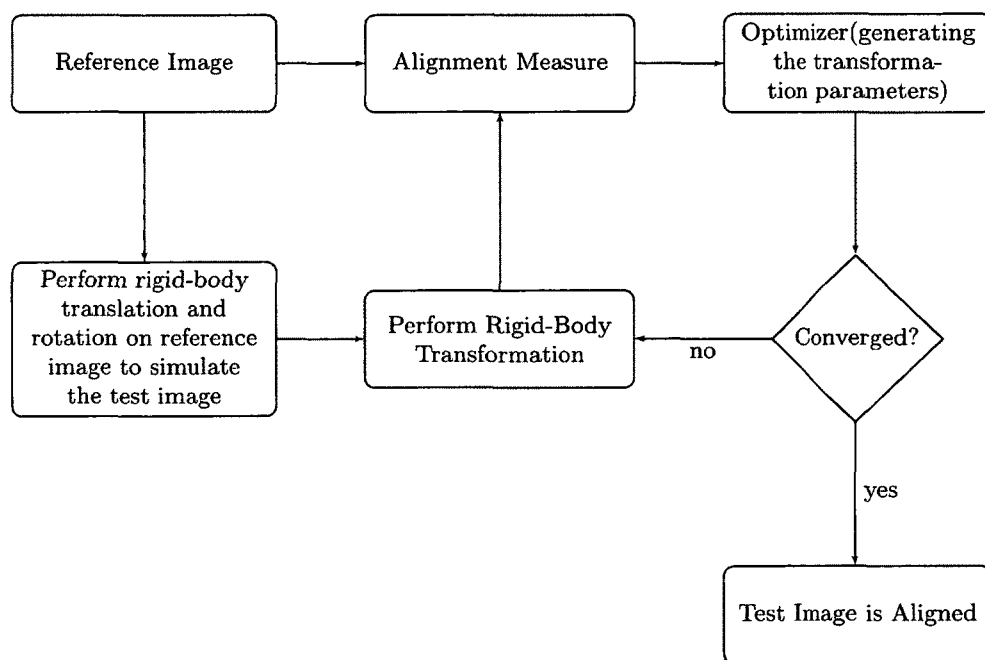


Figure 2.1: Flowchart of image registration stages in this thesis

In the following sections we will see how the rigid body transformation simulates the testing images. Further the various alignment measures which are based on divergence measure and mutual information will be explained. In the end we are going to

look at the `fminsearch` optimization algorithm which is based on the Downhill simplex optimization method.

## 2.2 Rigid-body Transformation

In this thesis we used two dimensional images because of the simplicity and the availability. We used the rigid-body transformation which refers to the transformations without shape distortion effects on images to be registered. Here the rigid-body transformation consists of rotation and horizontal and vertical translation. Any transformation consists of two stages. First is the transformation coordinate formation using the transformation matrix. Second is the interpolating the pixels to the new coordinates.

The algorithm which is used in this thesis for rigid-body transformation is as follows:

Step1: First we make  $x$  and  $y$  axis coordinates matrices using the `meshgrid` function in MATLAB. For instance for an image with three rows and three columns the  $x$  and  $y$  coordinate matrices are as follows:

$$\begin{bmatrix} 1 & 2 & 3 \\ 1 & 2 & 3 \\ 1 & 2 & 3 \end{bmatrix} \begin{bmatrix} 1 & 2 & 3 \\ 1 & 2 & 3 \\ 1 & 2 & 3 \end{bmatrix}$$

Figure 2.2: Right: matrix of  $x$  coordinate (`xcoords`) Left: matrix of  $y$  coordinate (`ycoords`)

Step 2: In this step we multiply the transformation matrix with the  $x$  and  $y$  coordinate matrices to form new coordinate matrices. For instance if there are 0.5 radius rotation and 2 cm translating on  $x$  and  $y$  axis, then the new  $x$  and  $y$  coordinates are calculated as follows:

$$xcoords_{new} = m11(xcoords - x_{center}) + m12(ycoords - y_{center}) + x_{offset},$$

$$ycoords_{new} = m21(xcoords - x_{center}) + m22(ycoords - y_{center}) + y_{offset}.$$

where

$$x_{center} = \frac{xsize}{xshift},$$

$$y_{center} = \frac{ysize}{yshift},$$

$$x_{offset} = x_{center} - x_{shift},$$

$$y_{offset} = y_{center} - y_{shift},$$

$$m11 = \cos(\text{angle}),$$

$$m12 = -\sin(\text{angle}),$$

$$m21 = -m12,$$

$$m22 = m11,$$

Here  $xsize = 3$  and  $ysize = 3$  and  $x_{shift} = 2$  and  $y_{shift} = 2$  may make a new coordinates which are rotated by 0.5 radius and translated on  $x$  and  $y$  axis by 2 cm.

Step 3: MATLAB function called "interp2" performs the interpolation. interp2 function receives the image matrix and the  $xcoords_{new}$  and  $ycoords_{new}$  and the type of the interpolation as input. The types of interpolation could be Nearest neighbor interpolation, Linear interpolation and Cubic spline interpolation. In this thesis we use the linear interpolation because we know there are no shape changes on the images.

## 2.3 Calculating the Alignment Measure

Among the alignment measures which are used for the area based rigid-body image registration, the joint histogram mutual information is one of the reference measures. The aim of this thesis is to develop a copula based divergence and mutual information measure based image registration algorithm and compare it with the joint histogram mutual information image registration.

There are various copula families in the literature [1]. Among available copula functions we chose four, out of which only Clayton copula from Archimedean family is used in image registration [14]. Four copula functions are Clayton, Frank, Gaussian, Marshal-Olkin [1]. The main reasons to chose these copulas are the simple form of alignment measure calculations and their interval of Kendall's tau.

In the following we will describe the joint histogram based mutual information and copula based divergence and mutual information measure concepts. These concepts are demonstrated by a simple example.

### 2.3.1 Joint Histogram Based Mutual Information

The mutual information registration alignment metric is known to be a powerful method in image registration [19]. In the year 1995 Colligon [18] and MIT group [16], started the use of mutual information in image registration. Considering Image  $A$  as the base image and image  $B$  as the image to be registered, the following equation will define the mutual information between images  $A$  and  $B$ :

$$I(A(x), B(x)) = H(A(x)) + H(B(x)) - H(A(x), B(x)), \quad (2.1)$$

where  $A(x)$  and  $B(x)$  are the intensity values matrices of images and  $H(A(x))$  and  $H(B(x))$  are the marginal entropies of images  $A$  and  $B$ .  $H(A(x), B(x))$  is the joint entropy of images  $A$  and  $B$ .

In Image registration the test image (Image  $B$ ) should be geometrically transferred until the maximum mutual information is obtained. Hence we can write the Equation (2.1) as follows:

$$I(A(x), T(B(x))) = H(A(x)) + H(T(B(x))) - H(A(x), T(B(x))), \quad (2.2)$$

where  $T(B(x))$  is the transformed version of image  $B$ . Therefore the value obtained from the Equation (2.2) is going to be used as the image registration alignment measure metric.

While working with images the joint histogram obtains the entropies for mutual information calculation. Joint histogram will find the frequencies of couple of intensities one from image  $A$  and another from image  $B$ . By dividing these frequencies by

the total number of pixels in any one of the images (since the reference and test images are of same size in this thesis), we will obtain the joint and marginal probability distributions.  $P(a_i, b_j)$  is the joint probabilities for images  $A$  and  $B$ .  $p(a_i)$  and  $p(b_j)$  are the marginal probabilities for the images  $A$  and  $B$  respectively. The following equation calculates the mutual information between images  $A$  and  $B$  using the joint and marginal probabilities of images  $A$  and  $B$ :

$$I(A, B) = \sum_i^q \sum_j^s P(a_i, b_j) \log \left[ \frac{P(a_i, b_j)}{p(a_i)p(b_j)} \right]. \quad (2.3)$$

To illustrate the steps used to calculate the joint histogram mutual information between two matrices, we use two 3 pixels by 3 pixels gray scale images and their corresponding intensity matrices which consist of three rows and three columns. The gray scale images have the intensity values between 0 and 255. Figure 2.3 shows two images and the corresponding matrices.

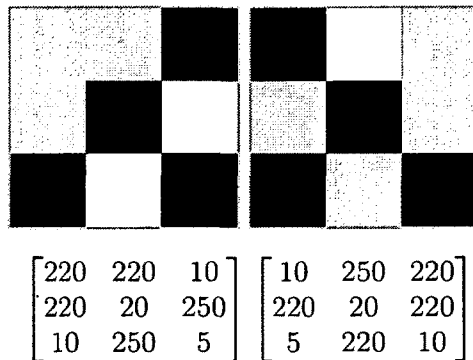


Figure 2.3: (Left: Image  $A$  Right: Image  $B$ ) Two gray scale images of size 3x3 and their corresponding intensity matrices below them

In the next step of calculating the mutual information we calculate the joint histogram for the two matrices in Figure 2.3 as follows:

Table 2.1: Joint Histogram of Image  $A$  and Image  $B$

A \ B	B					$p(a_i)$
	5	10	20	220	250	
5	0	$\frac{1}{9}$	0	0	0	$\frac{1}{9}$
10	$\frac{1}{9}$	0	0	$\frac{1}{9}$	0	$\frac{2}{9}$
20	0	0	$\frac{1}{9}$	0	0	$\frac{1}{9}$
220	0	$\frac{1}{9}$	0	$\frac{1}{9}$	$\frac{1}{9}$	$\frac{3}{9}$
250	0	0	0	$\frac{2}{9}$	0	$\frac{2}{9}$
$p(b_j)$	$\frac{1}{9}$	$\frac{2}{9}$	$\frac{1}{9}$	$\frac{4}{9}$	$\frac{1}{9}$	$\frac{9}{9}$

In the Table 2.1 the values on the margins are the marginal probabilities and the values in the central cells are the joint probabilities. In the following, mutual information for image  $A$  and image  $B$  is calculated using Equation (2.1):

$$\begin{aligned}
 I(A, B) &= \frac{1}{9} \log \frac{\frac{1}{9}}{\frac{2}{81}} + \frac{1}{9} \log \frac{\frac{1}{9}}{\frac{2}{81}} + \frac{1}{9} \log \frac{\frac{1}{9}}{\frac{8}{81}} + \frac{1}{9} \log \frac{\frac{1}{9}}{\frac{1}{81}} \\
 &\quad + \frac{1}{9} \log \frac{\frac{1}{9}}{\frac{6}{81}} + \frac{1}{9} \log \frac{\frac{1}{9}}{\frac{12}{81}} + \frac{1}{9} \log \frac{\frac{1}{9}}{\frac{3}{81}} + \frac{2}{9} \log \frac{\frac{2}{9}}{\frac{8}{81}} \\
 &= 0.9068,
 \end{aligned}$$

The mutual information between Image  $A$  and image  $B$  is 0.9068. This value will be used as the alignment measure between image  $A$  and image  $B$ .

### 2.3.2 Copula Based Alignment Measure

Copulas are functions which join uniform marginal distributions of random variables to form their multivariate distribution functions. Copulas separate joint distributions for two contributions: (i) marginal distributions of each variable and (ii) copula as a measure of dependence. Sklar's theorem [20] states that any multivariate distribution can be expressed as the  $k$ -copula function  $C(u_1, \dots, u_i, \dots, u_k)$  evaluated at each of the marginal distributions. Copula is not unique unless the marginal distributions are continuous. Using probability integral transform, each continuous marginal  $U_i = F_i(x_i)$  has a uniform distribution on  $I \in [0, 1]$  where  $F_i(x_i)$  is the cumulative integral of  $f_i(x_i)$  for the random variable  $X_i \in (-\infty, \infty)$ . The  $k$ -dimensional probability distribution function  $F$  has a unique copula representation

$$F(x_1, x_2, \dots, x_k) = C(F_1(x_1), F_2(x_2), \dots, F_k(x_k)) = C(u_1, u_2, \dots, u_k). \quad (2.4)$$

The joint probability density function is

$$f(x_1, x_2, \dots, x_k) = \prod_{i=1}^k f_i(x_i) c(F_1(x_1), F_2(x_2), \dots, F_k(x_k)), \quad (2.5)$$

where  $f_i(x_i)$  is each marginal density and coupling is provided by copula density

$$c(u_1, u_2, \dots, u_k) = \frac{(\partial^k C(u_1, u_2, \dots, u_k))}{(\partial u_1 \partial u_2 \dots \partial u_k)}, \quad (2.6)$$

if it exists. In case of independent random variables, copula density  $c(u_1, u_2, \dots, u_k)$  is identically equal to one. The importance of the above equation  $f(x_1, x_2, \dots, x_k)$  is that the independent portion expressed as the product of the marginals can be sepa-

rated from the function  $c(u_1, u_2, \dots, u_k)$  describing the dependence structure or shape. The dependence structure summarized by a copula is invariant under increasing and continuous transformations of the marginals.

The simplest copula is independent copula

$$\Pi := C(u_1, u_2, \dots, u_k) = u_1 u_2 \dots u_k, \quad (2.7)$$

with uniform density functions for independent random variables.

An empirical copula may be estimated from the  $N$  pairs of data  $(x_{1;t}, x_{2;t})_{0 < t \leq N}$  by

$$C(n/N, m/N) = \sum_t \mathbf{1}_{r_{t,1} \leq n, r_{t,2} \leq m}, \quad (2.8)$$

where  $r_{t,1}$  and  $r_{t,2}$  are the rank statistics of  $[x_{1;t}]_t$  and  $[x_{2;t}]_t$  respectively. Frecht [21] Hoeffding [22] lower and upper bounds for copula are respectively

$$W(u_1, u_2, \dots, u_k) := \max(1 - n + \sum_i u_i, 0) \leq C(u_1, u_2, \dots, u_k), \quad (2.9)$$

$$C(u_1, u_2, \dots, u_k) \leq \min_{i \in [1, 2, \dots, k]} u_i = M(u_1, u_2, \dots, u_k). \quad (2.10)$$

Relationships between copula and concordance measures Kendall's  $\tau$ , Spearman's  $\rho$ , Gini's index  $\gamma$  are as follows:

$$\tau = 4 \int \int_{I^2} C(u_1, u_2) dC(u_1, u_2) - 1, \quad (2.11)$$

$$\rho = 12 \int \int_{I^2} u_1 u_2 dC(u_1, u_2) - 3, \quad (2.12)$$

$$\gamma = 2 \int \int_{I^2} (|u_1 + u_2 - 1| - |u_1 - u_2|) dC(u_1, u_2). \quad (2.13)$$

In probability theory and statistics, a copula can be used to describe the dependence between random variables. They express joint structure among random variables with any marginal distributions.

The dependence between two sets of random variables can be calculated in terms of divergence measure. In this thesis for Clayton and Frank copulas, we used Kolmogorov copula based divergence to calculate the copula based divergence measure. Kolmogorov divergence is given in terms of copula density function as follows:

$$I(X, Y) = \iint_{[0,1]^2} |c(x, y) - 1| dy dx, \quad (2.14)$$

where  $c(x, y)$  is the copula density function. The copula density functions are obtained by performing differentiation on the copula distribution functions.

It is very important to choose the right copula function. One of the constraints to choose the appropriate copula is the interval of the copula parameters. As we will see in chapter 3, for the used data (MRI and Aerial images), four copula functions satisfied the copula parameter ( $\theta$ ) interval. The four copula functions and their family

names which are used in this thesis:

- i. Clayton from the Archimedean family.
- ii. Frank copula from Archimedean family.
- iii. Marshal-Olkin copula from non-Archimedean copula family with simultaneous presence of an absolutely continuous and a singular component.
- iv. Gaussian copula from elliptical family.

Here we present copula density function of each copula family and the calculation of the copula parameter in terms of Kendall's Tau.

## Clayton Copula

The Clayton copula cumulative distribution function (cdf) is provided in Equation (2.15) and it is plotted in Figure 2.4.

$$C(x, y) = (x^{-\theta} + y^{-\theta} - 1)^{-\frac{1}{\theta}}, \quad (2.15)$$

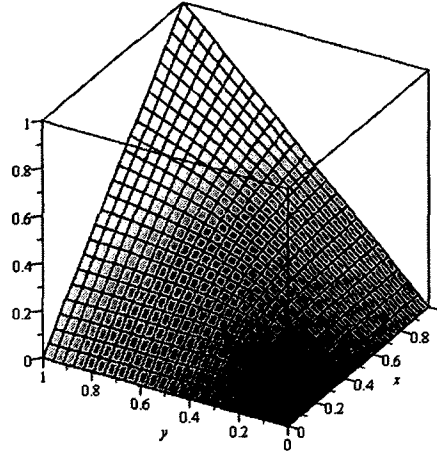


Figure 2.4: Clayton copula cumulative distribution function

where  $x$  and  $y$  are random variables between 0 and 1 and  $\theta$  is ( $0 < \theta < \infty$ ). After performing the Equation (2.6), we will obtain the Clayton copula probability density function (pdf) as:

$$c(x, y) = (1 + \theta)x^{-1-\theta}y^{-1-\theta}(-1 + x^{-\theta} + y^{-\theta})^{-2-\left(\frac{1}{\theta}\right)}, \quad (2.16)$$

where  $x$  and  $y$  are random variables between 0 and 1 and  $\theta$  is ( $0 < \theta < \infty$ ).  $c(x, y)$  is the Clayton copula density function. The relationship between Clayton copula parameter  $\theta$  and Kendalls rank correlation  $\tau$  is:

$$\theta = \frac{2\tau}{1 - \tau}, \quad (2.17)$$

where  $\tau$  is ( $0 \leq \tau < 1$ ) and  $\theta$  is ( $0 < \theta < \infty$ ).

In Figure 2.5 we can see the density curves of the Clayton copula for  $\theta = 0.1$  (first row left),  $\theta = 0.4$  (first row right) and  $\theta = 0.9$  (second row). Smaller  $\theta$  values represent weaker association and as the  $\theta$  value increases the association gets stronger. Figure 2.5 shows how the shape of Clayton copula density curve changes as the association gets stronger.

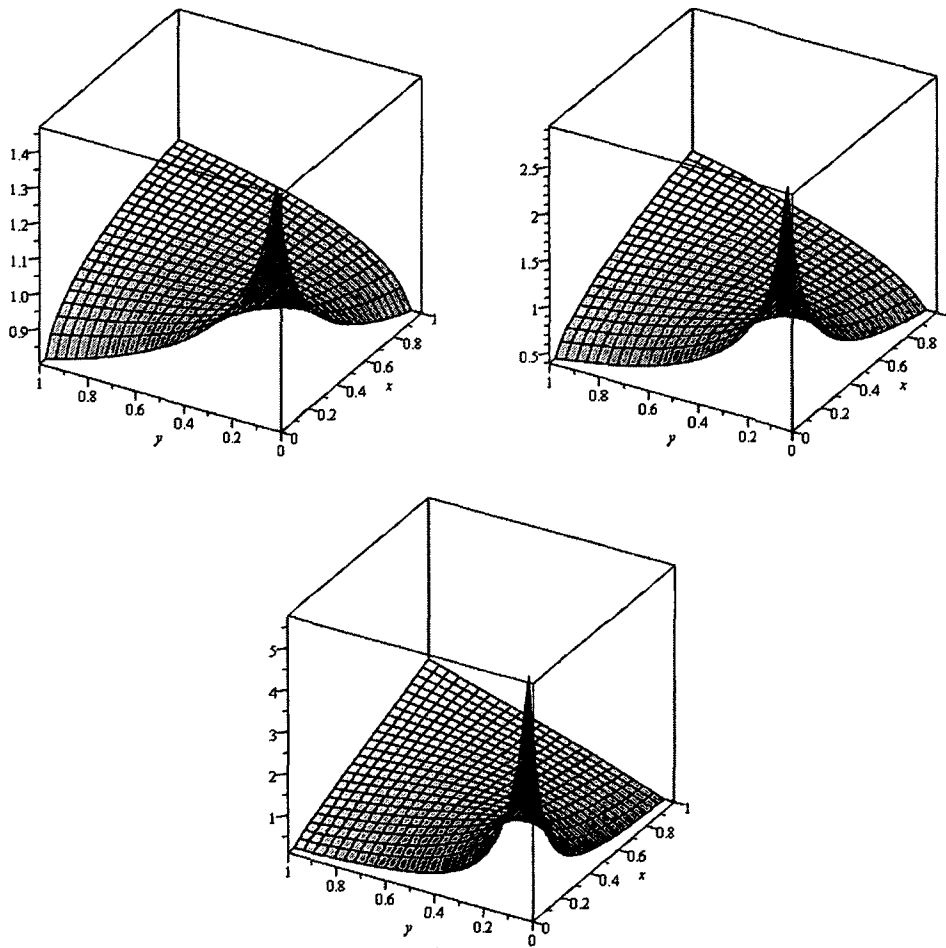


Figure 2.5: Clayton copula Probability density curves for  $\theta = 0.1$  (first row left),  $\theta = 0.4$  (first row right) and  $\theta = 0.9$  (second row)

## Frank Copula

The Frank copula cumulative distribution function (cdf) is provided in Equation (2.18) and it is plotted in Figure 2.6.

$$C(x, y) = -\frac{1}{\theta} \ln \left( 1 + \frac{(e^{-\theta x} - 1)(e^{-\theta y} - 1)}{(e^{-\theta} - 1)} \right), \quad (2.18)$$

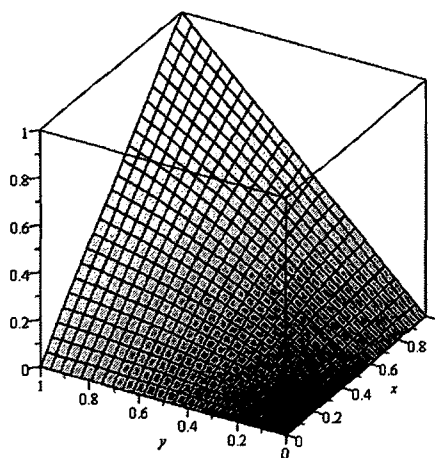


Figure 2.6: Frank copula cumulative distribution function

where  $x$  and  $y$  are random variables between 0 and 1 and  $\theta$  is  $(-\infty < \theta < \infty)$ . After performing the Equation (2.6), we will obtain the Frank copula probability density function (pdf) as:

$$c(x, y) = -\frac{e^{-\theta x} \theta e^{-\theta y} (e^{-\theta} - 1)}{(e^{-\theta x} (e^{-\theta y} - 1) + e^{-\theta} - e^{-\theta y})^2}, \quad (2.19)$$

where  $x$  and  $y$  are random variables between 0 and 1 and  $\theta$  is  $(-\infty < \theta < \infty)$ .  $c(x, y)$  is the Frank copula density function. The relationship between Frank copula

parameter  $\theta$  and Kendall's rank correlation  $\tau$  is:

$$\tau = 1 - \frac{4}{\theta^2} \int_0^\theta \frac{t}{e^{-t} - 1} dt, \quad (2.20)$$

where  $\tau$  is  $(-1 \leq \tau \leq 1)$  and  $\theta$  is  $(-\infty < \theta < \infty)$ .

In Figure 2.7 we can see the density curves of the Frank copula for  $\theta = 0.1$  (first row left),  $\theta = 0.4$  (first row right) and  $\theta = 0.9$  (second row). Smaller  $\theta$  values represent weaker association and as the  $\theta$  value increases the association gets stronger. Figure 2.7 shows how the shape of Frank copula density curve changes as the association gets stronger.

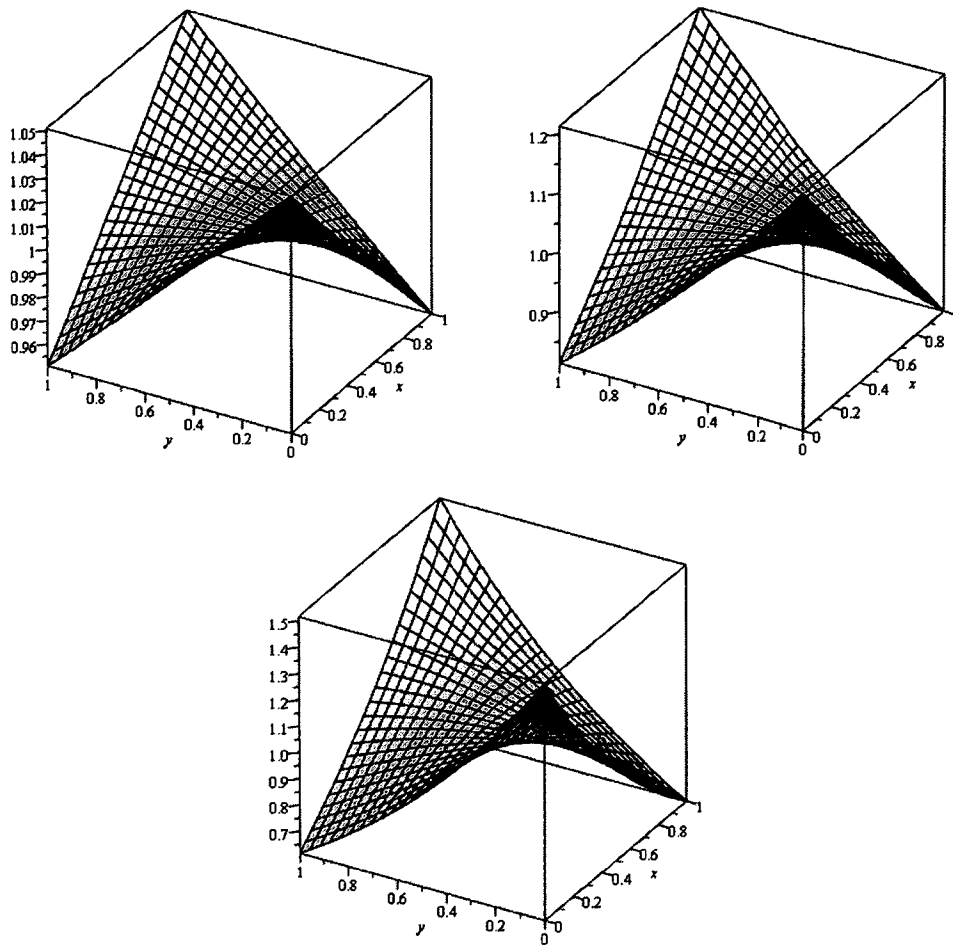


Figure 2.7: Frank copula Probability density curves for  $\theta = 0.1$  (first row left),  $\theta = 0.4$  (first row right) and  $\theta = 0.9$  (second row)

## Marshal-Olkin Copula

The Marshal-Olkin copula cumulative distribution function (cdf) is provided in Equation (2.21) and it is plotted in Figure 2.8.

$$C(x, y) = \min(x^{1-\theta}y, xy^{1-\theta}), \quad (2.21)$$

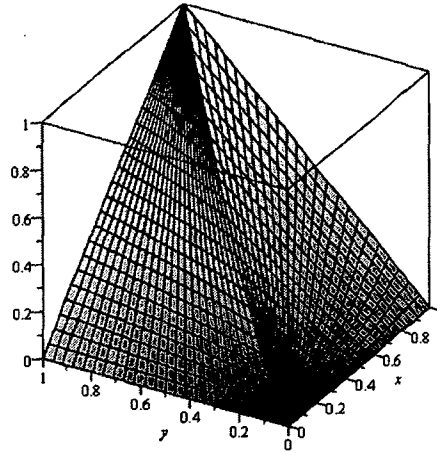


Figure 2.8: Marshal-Olkin copula cumulative distribution function

where  $x$  and  $y$  are random variables between 0 and 1 and  $\theta$  is ( $0 < \theta < 1$ ). After performing the Equation (2.6), we will obtain the Marshal-Olkin copula probability density function (pdf) as:

$$c(x, y) = \begin{cases} (1 - \theta)x^{-\theta} & \text{if } y < x \\ (1 - \theta)y^{-\theta} & \text{if } x < y, \end{cases} \quad (2.22)$$

where  $x$  and  $y$  are random variables between 0 and 1 and  $\theta$  is ( $0 < \theta < 1$ ).  $c(x, y)$  is the Marshal-Olkin copula density function. The relationship between Marshal-Olkin copula parameter  $\theta$  and Kendalls rank correlation  $\tau$  is:

$$\theta = \frac{2\tau}{1 + \tau}, \quad (2.23)$$

where  $\tau$  is ( $0 \leq \tau \leq 1$ ) and  $\theta$  is ( $0 < \theta < 1$ ).

In Figure 2.9 we can see the density curves of the Marshal-Olkin copula for  $\theta = 0.1$  (first row left),  $\theta = 0.4$  (first row right) and  $\theta = 0.9$  (second row). Smaller  $\theta$  values represent weaker association and as the  $\theta$  value increases the association gets stronger. Figure 2.9 shows how the shape of Marshal-Olkin copula density curve changes as the association gets stronger.

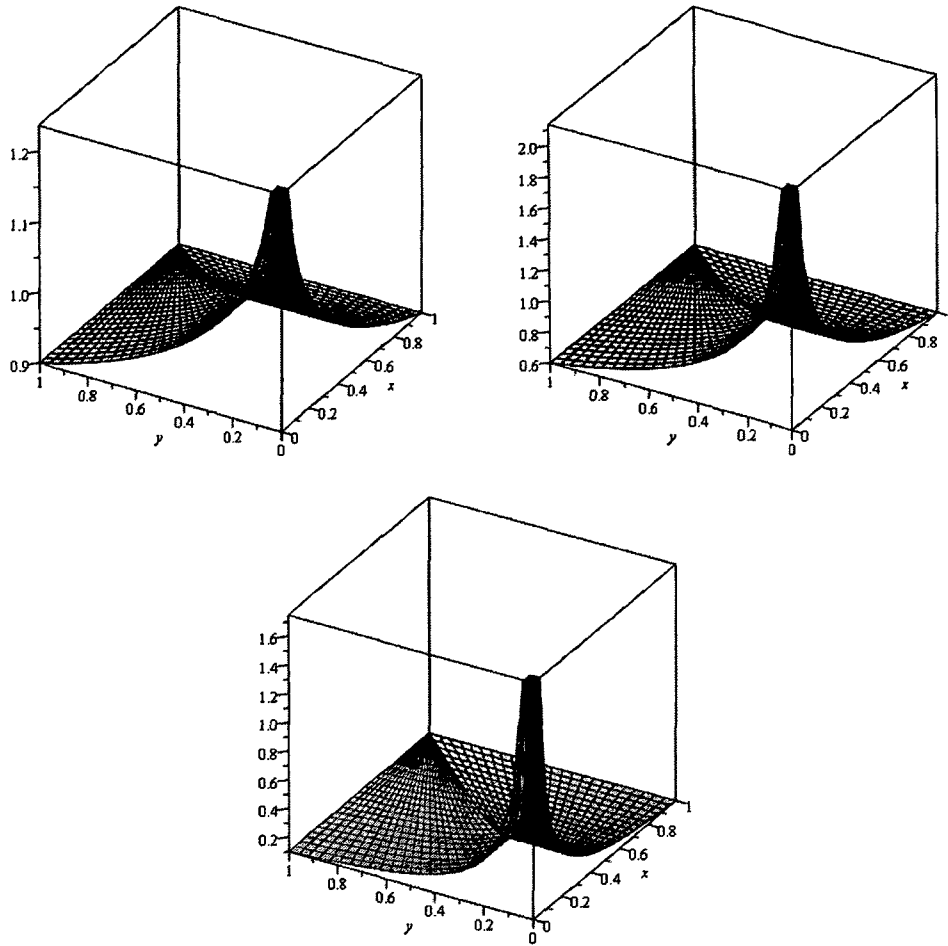


Figure 2.9: Marshal-Olkin copula Probability density curves for  $\theta = 0.1$  (first row left),  $\theta = 0.4$  (first row right) and  $\theta = 0.9$  (second row)

## Gaussian Copula

The Gaussian copula cumulative distribution function (cdf) is provided in Equation (2.24) and it is plotted in Figure 2.10.

$$C(x, y) = \int_{-\infty}^{\Phi^{-1}(x)} \int_{-\infty}^{\Phi^{-1}(y)} \frac{1}{2\pi\sqrt{1-\rho^2}} \exp\left(\frac{2\rho x_{in}y_{in} - x_{in}^2 - y_{in}^2}{2(1-\rho^2)}\right) dx dy, \quad (2.24)$$

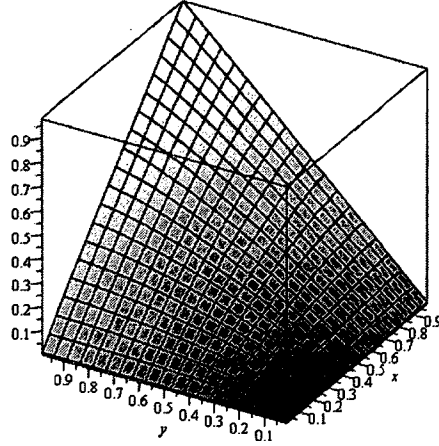


Figure 2.10: Gaussian copula cumulative distribution function

where  $x$  and  $y$  are random variables between 0 and 1 and  $\rho$  is  $(-1 < \rho < 1)$  and  $x_{in} = \Phi^{-1}(x)$  and  $y_{in} = \Phi^{-1}(y)$ . After performing the Equation (2.6), we will obtain the Gaussian copula probability density function (pdf) as:

$$c(x, y) = (1 - \rho^2)^{-\frac{1}{2}} \exp\left(-\frac{1}{2}(1 - \rho^2)^{-1}(x_{in}^2 + y_{in}^2 - 2\rho x_{in}y_{in})\right) \exp\left(\frac{1}{2}(x_{in}^2 + y_{in}^2)\right), \quad (2.25)$$

where  $x$  and  $y$  are random variables between 0 and 1 and  $\rho$  is  $(-1 < \rho < 1)$ .  $x_{in} = \Phi^{-1}(x)$  and  $y_{in} = \Phi^{-1}(y)$  and  $c(x, y)$  is the Gaussian copula density function. Here  $\phi \in [-1, 1]$  is the parameter of Gaussian copula and  $\Phi^{-1}$  is the inverse standard Gaussian cumulative distribution function. The relationship between Gaussian copula parameter  $\rho$  and Kendalls rank correlation  $\tau$  is:

$$\rho = \sin\left(\frac{\pi}{2\tau}\right), \quad (2.26)$$

where  $\tau$  is  $(-1 < \tau < 1)$  and  $\rho$  is  $(-1 < \rho < 1)$ .

In Figure 2.11 we can see the density curves of the Gaussian copula for  $\rho = 0.1$  (first row left),  $\rho = 0.4$  (first row right) and  $\rho = 0.9$  (second row). Smaller  $\rho$  values represent weaker association and as the  $\rho$  value increases the association gets stronger. Figure 2.11 shows how the shape of Gaussian copula density curve changes as the association gets stronger.

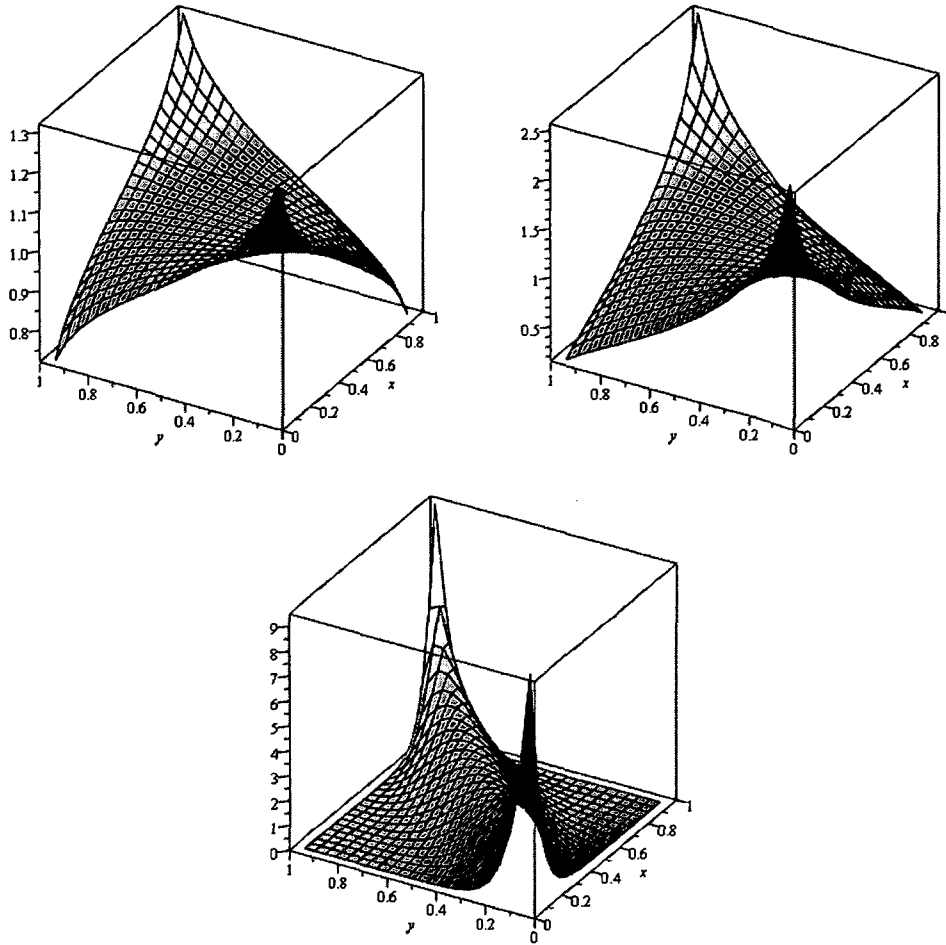


Figure 2.11: Gaussian copula Probability density curves for  $\rho = 0.1$  (first row left),  $\rho = 0.4$  (first row right) and  $\rho = 0.9$  (second row)

### 2.3.3 Examples of Copula Based Alignment Measure

Clayton and Frank copula density functions are used in the Equation (2.14) in order to calculate the copula based divergence as alignment measure. Equation (2.14)

is the Kolmogorov copula based divergence measure which finds the divergence between two random variables. There are various copula based divergence functions such as Kullback-Leibler, Tsallis, Renyi and Kolmogorov. In this thesis we use the Kolmogorov copula based divergence measure due to its simplicity and faster calculation.

For Marshal Olkin and Gaussian copulas the mutual information is provided in Equations (2.27) and (2.28) respectively. Marshal Olkin and Gaussian based mutual information metrics are used as alignment measures. Here we use the mutual information measure for Marshal Olkin and Gaussian copulas since the simple forms are provided.

$$I(x, y) = \frac{-2 + 2\theta}{2 - \theta} \log(1 - \theta) + \frac{\theta}{2 - \theta}, \quad (2.27)$$

where  $\theta$  is Marshal Olkin copula parameter from Equation (2.23).

$$I(x, y) = \frac{-1}{2} \log(1 - \rho^2), \quad (2.28)$$

where  $\rho$  is the Pearson correlation between the two random variables  $x$  and  $y$ .

In Figure 2.12 we can see the calculated divergence and mutual information values between two random numbers using the Clayton, Frank, Marshal and Gaussian copulas. Here we observed that divergence measure does not exist for Clayton copula for  $\tau > 0.8$ . Also mutual information decreases for Marshal Olkin for  $\tau > 0.8$ . In Figure 2.12 and Table 2.2, we use the Pearson correlation for the presentation purpose.

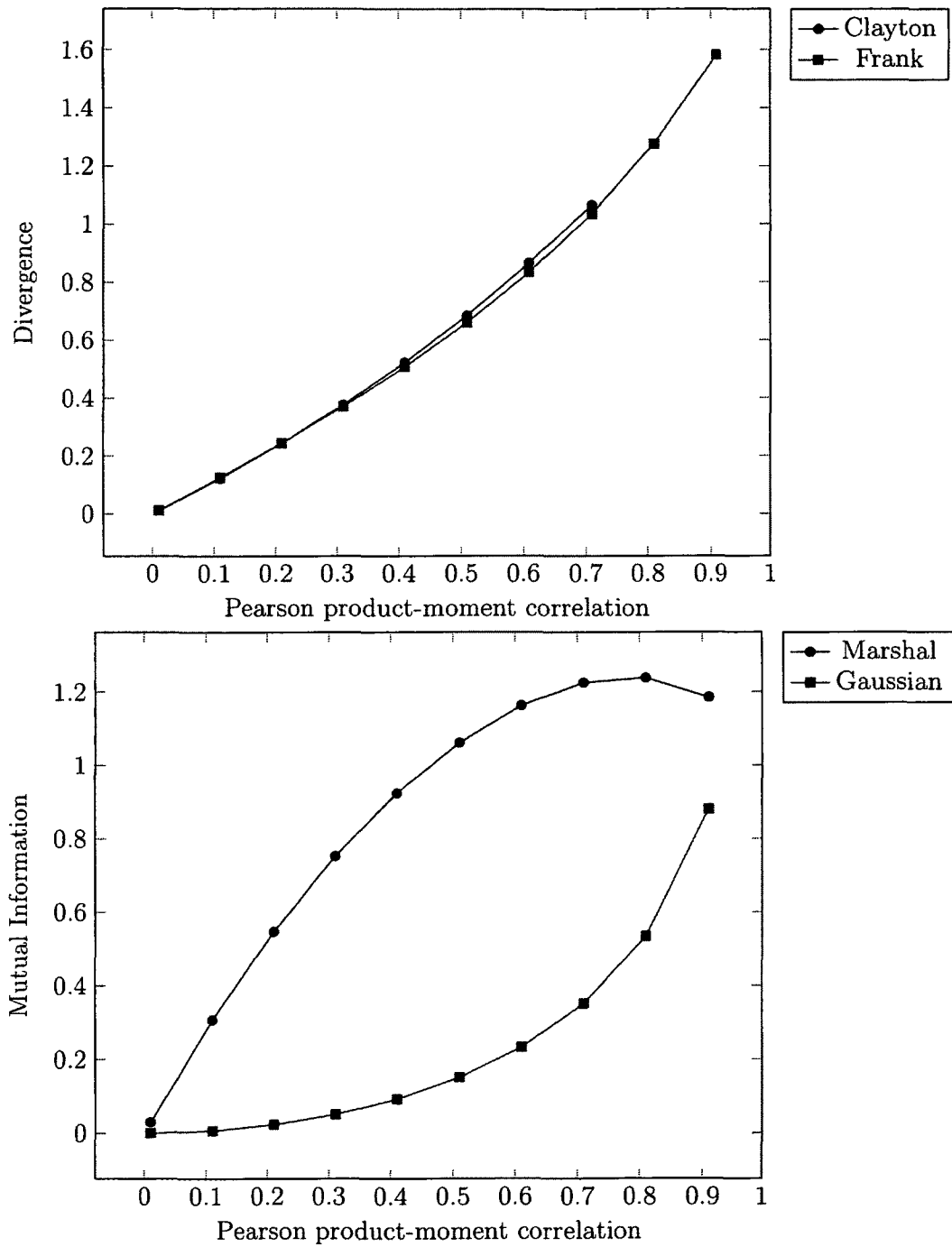


Figure 2.12: Divergence measures and mutual information calculated using four copulas

The values of divergence measure and mutual information calculated using Clayton, Frank, Marshal-Olkin and Gaussian copulas are presented in Table 2.2.

Table 2.2: Values of the divergence measures and mutual information in Figure 2.4

Pearson Correlation	Marshal	Clayton	Frank	Gaussian
0.010	0.030	0.011	0.011	0.000
0.110	0.307	0.122	0.125	0.006
0.210	0.547	0.243	0.244	0.023
0.310	0.752	0.376	0.370	0.051
0.410	0.924	0.522	0.507	0.092
0.510	1.061	0.684	0.660	0.151
0.610	1.163	0.865	0.832	0.233
0.710	1.225	1.065	1.034	0.351
0.810	1.238	NaN	1.276	0.534
0.910	1.185	NaN	1.583	0.880

Now we shall demonstrate an example which shows the calculation of copula based divergence measure and mutual information using the Equation (2.14). Let us use the sample images in Figure 2.3. The following are the steps to calculate the divergence measure using the Frank copula density in Kolmogorov divergence function:

Step1: Here we arrange pixels for both the images in Figure 2.3 in column matrices. In order to make the column matrix we have to append each column of the matrix to the end of the first column (Figure 2.13).

Step 2: In this step we calculate the Kendall's Tau rank correlation between the two column matrices.

$$\tau = 0.4336,$$

220	10
220	220
10	5
220	250
20	20
250	220
10	220
250	220
5	10

Figure 2.13: Left: Column matrix of Image A Right Column matrix of Image B

Step 3: Using Equation (2.20) to calculate the Frank copula parameter  $\theta$  using the Kendall's Tau.

$$\theta = 4.6433,$$

Step 4: Using the Equation (2.14), in this step we calculate the double integration of the Frank density function with the calculated copula parameter:

$$I(X, Y) = \iint_{[0,1]^2} \left| \left( -\frac{e^{-\theta x} \theta e^{-\theta y} (e^{-\theta} - 1)}{(e^{-\theta x} (e^{-\theta y} - 1) + e^{-\theta} - e^{-\theta y})^2} \right) - 1 \right| dy dx = 0.54185,$$

The divergence measure of images  $A$  and  $B$  in Figure 2.3 by using the Frank copula based Kolmogorove divergence is 0.54185.

The Clayton copula based divergence measure also calculated using the same four steps as Frank copula (in steps 3 and 4 we use the Clayton copula parameter and density function) . For Marshal-Olkin and Gaussian copulas the calculations are simpler.

In Marshal-Olkin copula after the step 3 and calculating the copula parameter using the Equation (2.23), we perform Equation (2.27) and find the mutual information between images  $A$  and  $B$ .

$$I(x, y) = \frac{-2 + 2\theta}{2 - \theta} \log(1 - \theta) + \frac{\theta}{2 - \theta} = 0.9596,$$

where  $\theta = \frac{2\tau}{1+\tau} = 0.6049$ .

In Gaussian copula we use the Pearson correlation between the two column matrices and calculate the mutual information using Equation (2.28) as follows:

$$I(x, y) = \frac{-1}{2} \log(1 - (\rho^2)) = 0.1993,$$

where  $\rho$  is the Pearson correlation between the two matrices and its value in this case is 0.5733.

## 2.4 Optimization

For the images which are similar and need few numbers of transformations to be registered, optimization is not required and this method is called direct image registration. Direct image registration uses the registration metric (alignment measure) and after few transformations, by reaching to the maximum or minimum metric the images get registered. On the other hand when the images are not similar and there are many numbers of transformations, the optimization is used in image registration algorithms. There are various optimization techniques of which we use the MATLAB `fminsearch` optimization method [23]. The `fminsearch` uses the Nelder-Mead

simplex method. The `fminsearch` is also called the direct search in which we search for the smallest scalar of a function iteratively. In this algorithm we are searching for the smallest scalar of alignment metric function. In this thesis the alignment metric function provides the negated value of divergence measure and mutual information. Higher values of divergence measure and mutual information are closer to the registration point, therefore `fminsearch` finds the maximum absolute value of them. In the Nelder-Mead search method we should provide the metric function, initial values of transformation and the predefined parameters. These parameters are the starting point of the transformations for image registration. After the initial transformation of the test image the alignment measure will be calculated between the transformed test image and reference image. The optimization algorithm will decide whether the alignment measure is optimum or not. The transformation will be continued with the transformation parameters from the optimization algorithm until the optimum alignment measure is found.

The `fminsearch` algorithm and the predefined parameters are obtained from the [23] paper and presented here. The predefined parameters are:

$$\rho = 1, \chi = 2, \gamma = \frac{1}{2}, \sigma = \frac{1}{2}, \quad (2.29)$$

By using the above parameters and based on the Nelder-Mead search algorithm constraints on the scalar value (negated divergence measure or mutual information), the passing transformation parameters to the metric function gets updated.

In the following we will see an example of the image registration of the Figure 2.3 by using the `fminsearch` and the joint histogram based mutual information as the alignment metric function. Here the left image in Figure 2.3 is the reference image

and the right image is the test image.

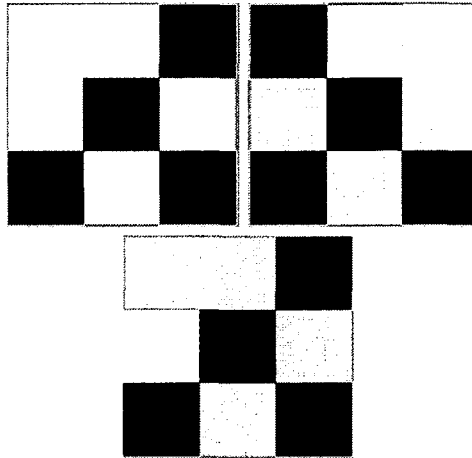


Figure 2.14: Left: Reference Image Right: Test Image bottom: Registered test image using the fminsearch and joint histogram based mutual information

By looking at Figure 2.14 we can observe that if we rotate the test image by 90 degree counter-clockwise, we can obtain the best possible registration. The fminsearch optimization algorithm is implemented in MATLAB and we obtained the transformation metric (90 degree) in 25 iterations. In these 25 iterations fminsearch refers to the alignment metric function to calculate the negated mutual information and finds the best transformation metric. Figure 2.15 shows the iterations and the values of the negated mutual information in each iteration.

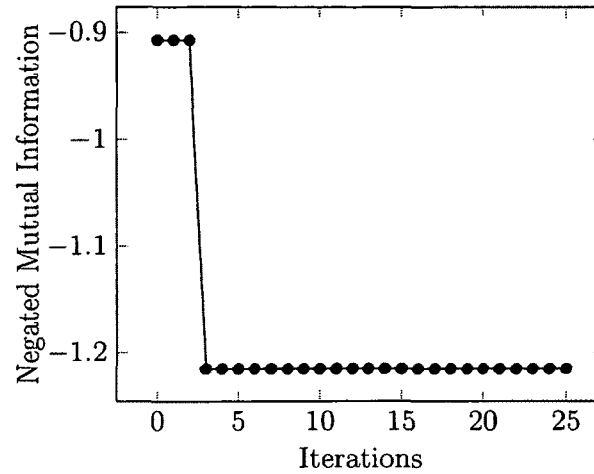


Figure 2.15: Plot of the convergence of the fminsearch in 25 iterations

Here we can see after 25 iterations the value of -1.21489 is chosen to be the minimum negated mutual information value and the  $x$  which is the transformation parameter is 90 degree. This means the counter clockwise rotation of 90 degree should be performed on the image  $B$  to be registered or aligned to image  $A$ .

# Chapter 3

## Experiments

In this chapter we will present the results of the experiments of copula based image registrations and compare them with the standard image registration method. These experiments are performed on the MRI and Aerial images. This chapter starts with the description about the images used in this thesis and continues with the results of the image registration for four copula functions namely, Clayton, Frank, Gaussian and Marshal- Olkin copulas. In the end we shall summarize the copula based image registration and the standard image registration (joint histogram) method's results.

### 3.1 Experimental Images

Two main applications of image registration are its use in medical and aerial image processing. Most of the medical images are in three dimensions. In the literature in order to test the performance of a new image registration metric they use a slice

of these three dimensional images [14]. These slices are of two dimension and are simpler and less time consuming, in comparison with the three dimension. In this thesis our aim is to monitor the performance of the copula based image registration and we are using the gray-scale two dimensional slices of the Magnetic Resonance Imaging (MRI) and aerial images. These gray-scale images contain the intensity values in the range of 0 to 255 in which 0 is white shade and as we move to 255 the shades get darker. The images are collected as the reference images and geometrical transformation algorithm has been applied on these reference images to generate the test images. The transformation algorithm to make the test images, consisted of 2 centimetres translation on  $x$  and  $y$  axis, and 0.5 radius counter-clockwise rotation. Simulation of test images, tells us the exact transformation factors and hence we can compare the results of the registration with the transformation factors. For instance now we know that if the registration algorithms obtain the geometrical transformation values as translation of -2 centimetres in  $x$  and  $y$  axis and rotation of -0.5 radius (clockwise) may provide the best possible registration.

### 3.1.1 Magnetic Resonance Imaging (MRI)

We use one slice gray scale of Magnetic Resonance Image (MRI) for 8 patients which are obtained from the Vanderbilt University's medical image research website [25]. These images are with Joint Photographic Experts Group (JPEG) format. In Figure 3.1 we can see the reference images  $P1$  (patient 1) to  $P8$  (patient 8) and the test images ( $TP1$  to  $TP8$ ) which are images from the same patients as  $P1$  to  $P8$ , translated 2 centimetres in  $x$  and  $y$  axis and rotated counter-clockwise 0.5 radius. These images are two dimensional with the resolution of 256 X 256. In the experiments of the MRI images we obtain a region of interest (ROI) of rectangular shape with coordinates:

$[x_1=30, y_1=30, x_2=225, y_2=225]$  and the calculations are performed on the region of interest. Region of interest may discard the unimportant portions of the image such as the background. We use the region of interest for the MRI images and not for the aerial images because all parts of the aerial images are important for image registration.

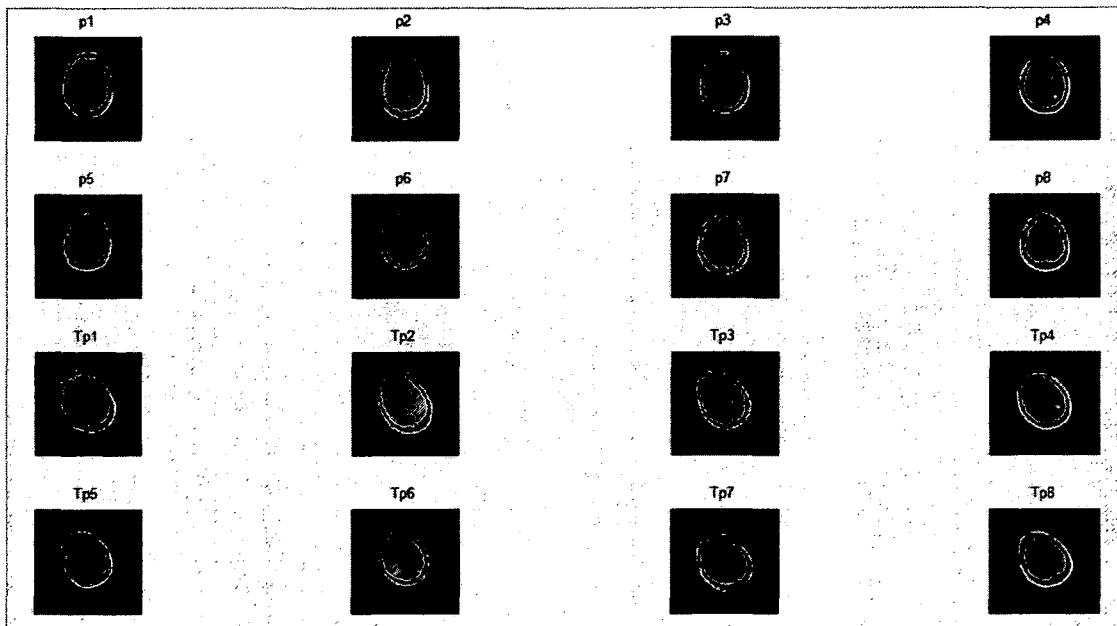


Figure 3.1: P1 to P8 are the reference images and TP1 to Tp8 are the testing images

## Aerial Images

Aerial images in this thesis are acquired from Quick Bird sensor (QUICKBIRD SATELLITE IMAGES) [24] with Joint Photographic Experts Group (JPEG) format. Eight 2-D gray scale aerial images are presented in the first two rows of Figure 3.2 and

labelled as A1 to A8. The description and the geographic location of these images are provided in Appendix B. These images originally were color images of resolution 512 X 512 X 3 . By using the MATLAB function called `rgb2gray()` we converted these images to gray scale images that are with resolution 512 X 512. With another MATLAB function called `imresize()` we down-sampled these images to 188 X 188 resolution for all the images except the seventh image (A7) which is of resolution 177 X 177. As one can see in the Figure 3.2, the images were padded on the margins which is called zero padding. In Figure 3.2 the images with labels A1 to A8 are the reference images and images with TA1 to TA8 are 2 centimetres translated on  $x$  and  $y$  axis and rotated 0.5 radius counted-clockwise version of the reference images. TA1 to TA8 are called the test images (moving images) in this thesis.

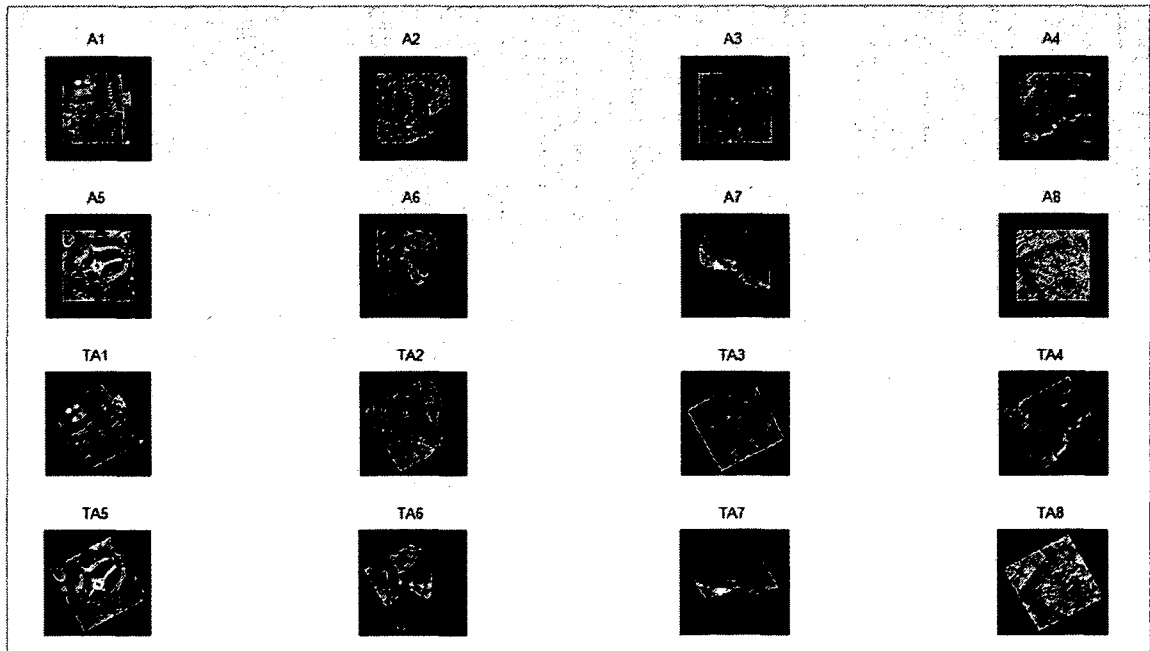


Figure 3.2: A1 to A8 are the reference images and TA1 to TA8 are the testing images

### 3.1.2 Which Copula ?

Before starting the experiments we had to check which copula function is appropriate for the images used in this thesis. In order to know which copula function is appropriate we shall obtain the Kendall's Tau intervals of the paired images (reference and test images) to see if atleast the initial intervals are with in the used copula's constraints. The four copula functions which are used in this thesis consist of the following constraints:

Gaussian copula:  $\tau$  is  $(-1 < \tau < 1)$  and  $\rho$  is  $(-1 < \rho < 1)$ .

Clayton copula:  $\tau$  is  $(0 \leq \tau < 1)$  and  $\theta$  is  $(0 < \theta < \infty)$ .

Marshal Olkin copula:  $\tau$  is  $(0 \leq \tau \leq 1)$  and  $\theta$  is  $(0 < \theta < 1)$ .

Frank copula:  $\tau$  is  $(-1 \leq \tau \leq 1)$  and  $\theta$  is  $(-\infty < \theta < \infty)$ .

Apart from the above conditions, as we saw in the previous chapter for  $\tau > 0.8$ , Marshal Olkin and Clayton copulas do not provide appropriate measures. Hence the appropriateness of copula functions must be investigated in the image registration experiments.

## 3.2 Results of Image Registration Experiments

As mentioned in the previous section we have sixteen cases of image registration from which eight are MRI images and eight are aerial images. At this section we are going to report the performance of the image registration of these sixteen images using the five distinct alignment measure methods. These five methods are joint histogram, Gaussian copula, Marshal-Olkin copula, Clayton copula and Frank copula. We shall measure the performance of these image registration methods by using the peak signal-

to-noise ratio (PSNR) method, in which the closer the value of PSNR to zero is, the better the performance of the image registration algorithm. The calculation of PSNR for two intensity matrices of two images is as follows:

$$PSNR = 10 \log_{10} \left[ \frac{1}{MSE} \right], \quad (3.1)$$

where MSE (Mean Square Error) is  $MSE = \frac{\sum_{X,Y} [I_1(x,y) - I_2(x,y)]^2}{XY}$ , and  $x$  and  $y$  are the numbers of pixels in each of the respective axis.  $I_1(x,y)$  and  $I_2(x,y)$  are the intensity values of image 1 and image 2.

As we discussed in chapter 2, the `fminsearch` optimization algorithm searches for the global minimum, hence we use the negated values of divergence measure and mutual information. Here the maximum value of negated values of divergence measure and mutual information will be the global minimum value for the `fminsearch` optimization algorithm. In this point the `fminsearch` algorithm converges and announces the obtained geometrical transformation values. When we transform the test image using the resulted value of geometrical transformation from the optimization algorithm, we are supposed to obtain an image in which the PSNR value is close to zero. If the PSNR value is close to zero, it means the tested image is nearest possible to the reference image. The header columns of the tables in this section from left to right report the following: (Tables 3.1, 3.2, 3.3, 3.4 and 3.5)

Column 1. Name of the images which are registered.

Column 2. Initial AM (Alignment Measure) is the negated divergence measure or mutual information between the reference and the test images before starting the reg-

istration algorithm.

Column 3. Final AM (Alignment Measure) is the final negated divergence measure or mutual information value which is the global minimum value that `fminsearch` converged for it and declared the corresponding transformations optimum.

Column 4. Final T is the final transformation that the image registration algorithm converges to it. The transformations are shown as three values in which from left to right, the first value is the translation on the  $x$  axis, second value is the translation on the  $y$  axis and the third value is the rotation angle in terms of radius.

Column 5. Iteration is the number of iterations in which the `fminsearch` algorithm converges.

Column 6. PSNR is peak signal-to-noise ratio between the registered test image and the reference image.

Also for all the registration algorithms we need to provide the initial values for the geometrical transformation in which we provided as 5 centimetres translation on  $x$  and  $y$  axis and 0.2 radius counter-clockwise rotation. Note that these initial values were provided in the literature [26] and we did not change them because of comparison of the new copula based image registration algorithm with the reported results in the literature.

In the following we will see the tabulated results of the proposed image registration methods.

### 3.2.1 Joint Histogram Mutual Information

The joint histogram mutual information based image registration is one of the popular methods in area based image registration. Hence here in fminsearch optimization method, the negated joint histogram mutual information is used as the objective or metric function (Alignment Measure) which guides the fminsearch optimization to converge and find the best possible geometrical transformation. The results of the joint histogram based image registration method are reported in Table 3.1.

Table 3.1: Image registration results for joint histogram mutual information

Images	InitialAM	FinalAM	FinalT	Iterations	PSNR
P1	-0.86	-2.07	(-2.0081 -2.0083 -0.5000)	59	-12.76
P2	-0.89	-2.08	(-1.9988 -2.0105 -0.5000)	85	-12.85
P3	-0.83	-2.08	(-2.0025 -2.0169 -0.5002)	71	-12.71
P4	-0.93	-2.08	(-1.9699 -2.0028 -0.5000)	78	-12.18
P5	-0.90	-2.13	(-2.0071 -2.0053 -0.5000)	61	-11.05
P6	-0.86	-2.00	(-2.0120 -2.0079 -0.5001)	84	-11.42
P7	-0.93	-2.14	(-1.9972 -1.9938 -0.5001)	82	-10.52
P8	-0.96	-2.12	(-2.0102 -2.0050 -0.5001)	69	-11.37
A1	-0.46	-0.99	(1.5018 3.2268 -0.4990)	84	-32.03
A2	-0.45	-1.74	(-2.0010 -2.0136 -0.5000)	72	-22.83
A3	-0.32	-1.51	(-1.9959 -1.9857 -0.5000)	79	-22.79
A4	-0.37	-1.68	( -2.0089 -1.9842 -0.4999)	75	-22.30
A5	-0.48	-1.75	(-2.0101 -2.0140 -0.5002)	74	-24.33
A6	-0.53	-1.95	(-1.9946 -1.9998 -0.5000)	74	-21.41
A7	-0.53	-2.18	(-2.0030 -1.9891 -0.5001)	72	-16.72
A8	-0.45	-1.73	(-2.0117 -1.9958 -0.4999)	76	-24.99

In Table 3.1 we observe the first aerial image (A1) is a miss-registered case, in which the PSNR value between the registered image and the reference image is very small (far from zero) and hence it is not registered properly. Also we can observe that the PSNR values of the MRI images are larger than the aerial images. This is because the corners of the aerial test images disappear while simulating them (effect of rotation on rectangular images in Figure 3.3). While registering, the corners of the aerial test images are missing which leads to smaller PSNR value in comparison with the MRI images. For MRI test images simulation there are no lost parts, since their background are black and does not have the effect of rotation on rectangular images. In Figure 3.3 we can see the first aerial miss-registered image. In this figure the red channel, belongs to the reference image and blue channel, belongs to the test image. Here the joint histogram based algorithm obtained the transformation which is  $(1.5018 \ 3.2268 \ -0.4990)$ . Here the test image is translated 1.5018 centimetres on  $x$  axis and 3.2268 centimetres on  $y$  axis and rotated  $-0.4990$  radius which is very far from the reference transformation values that should be close to  $(-2, -2, -0.5)$ .

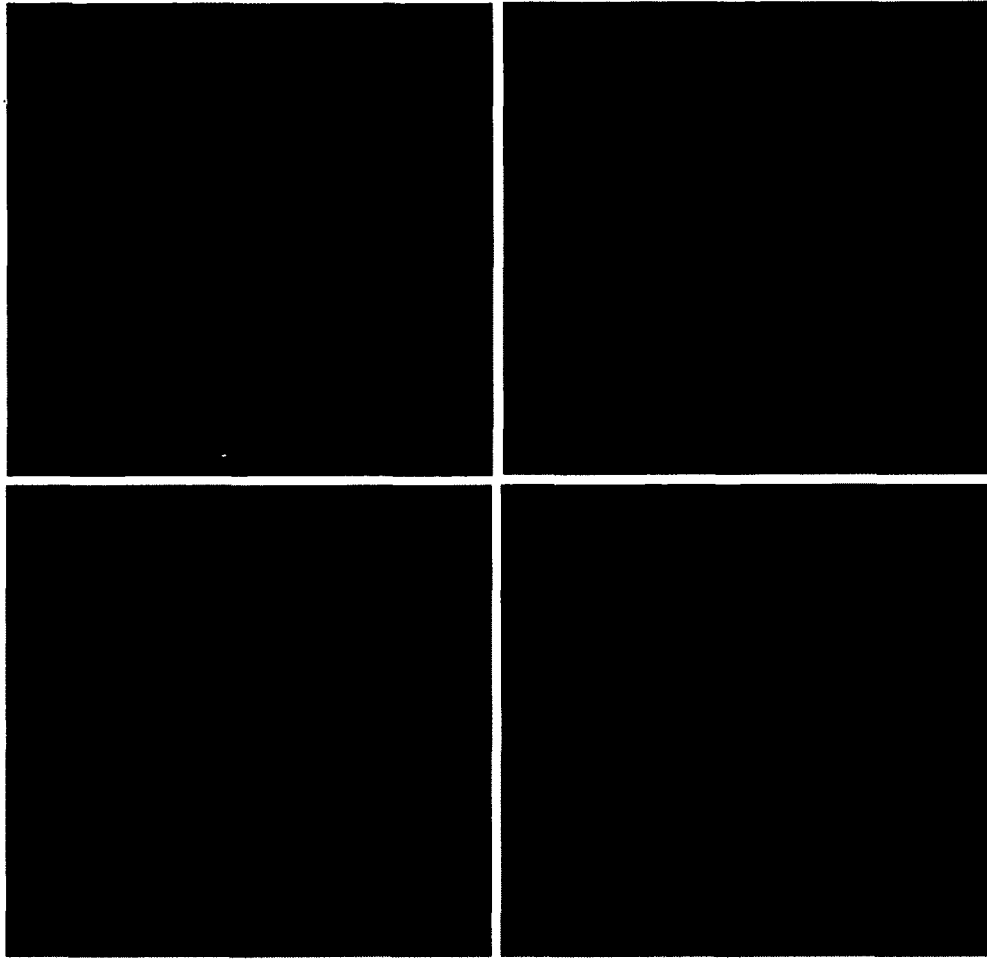


Figure 3.3: First aerial image which mis-registered using the joint histogram mutual information method. (First row left: the reference image, first row right: the test image, second row left: the registered test image, second row right: the overlap of registered test image on the reference image which is mis-registered)

### 3.2.2 Clayton Copula

Clayton copula is from Archimedean copula family. It is one of the registration alignment metric functions, which may lead the test images to get aligned to the reference

images. Here the alignment measure is the negated Kolmogorove divergence measure. As we can see in the Table 3.2 the PSNR values of this method are lower than the other four methods (far from zero). Also we can see in Final Am column, the values are -1.26 which indicates that  $\tau > 0.8$ , (section 2.3.3) where the divergence measure does not exist for the Clayton copula and the optimization algorithm stops at this point. Hence the combination of Clayton copula and fminsearch optimization was not successful in registering the images in this thesis.

Table 3.2: Image registration results for Clayton Copula

Images	InitialAM	FinalAM	FinalT	Iterations	PSNR
P1	-0.64	-1.26	(-1.5478 -2.2116 -0.5068)	72	-17.65
P2	-0.69	-1.26	(-2.6049 -1.6625 -0.5025)	78	-19.17
P3	-0.67	-1.26	(-2.3662 -1.8764 -0.4910)	69	-17.57
P4	-0.67	-1.26	(-2.0666 -2.7114 -0.4999)	61	-18.41
P5	-0.68	-1.26	(-1.9466 -1.2580 -0.4969)	53	-17.78
P6	-0.71	-1.26	(-1.4237 -2.5233 -0.4993)	50	-18.46
P7	-0.72	-1.26	(-2.5197 -2.3777 -0.5088)	35	-16.53
P8	-0.69	-1.26	(-1.6440 -1.4109 -0.5004)	36	-16.56
A1	-0.49	-1.26	(-1.5507 -0.3933 -0.4961)	70	-28.12
A2	-0.47	-1.26	(-1.7790 -0.8507 -0.4936)	70	-28.61
A3	-0.43	-1.26	(-1.4453 -2.1648 -0.4929)	87	-24.91
A4	-0.43	-1.26	(-2.4282 -0.2177 -0.5096)	99	-26.61
A5	-0.36	-1.26	(-1.5795 -2.0429 -0.5140)	77	-28.98
A6	-0.60	-1.26	(1.6422 1.3176 -0.4720)	56	-29.85
A7	-0.65	-1.26	(0.7547 1.5196 -0.4670)	71	-27.52
A8	-0.37	-1.26	(-2.8610 -2.0608 -0.5052)	88	-29.54

### 3.2.3 Frank Copula

Frank copula is from Archimedean copula family, which is used as the registration metric function in fminsearch optimization. Here the alignment measure is the negated Kolmogorove divergence measure. Table 3.3 shows the results of the 16 cases of image registration. The performance of Frank copula was satisfactory because the PSNR values are closer to zero.

Table 3.3: Image registration results for Frank Copula

Images	InitialAM	FinalAM	FinalT	Iterations	PSNR
P1	-0.54	-1.58	(-1.9952 -1.9982 -0.5000)	67	-12.76
P2	-0.58	-1.58	(-2.0020 -1.9985 -0.5000)	72	-12.84
P3	-0.57	-1.58	(-1.9951 -1.9984 -0.5000)	71	-12.71
P4	-0.57	-1.56	(-1.9982 -2.0026 -0.4999)	92	-12.14
P5	-0.57	-1.60	(-2.0005 -1.9982 -0.5000)	94	-11.05
P6	-0.59	-1.56	(-2.0003 -2.0026 -0.4999 )	80	-11.41
P7	-0.60	-1.61	(-1.9994 -1.9997 -0.5000)	67	-10.52
P8	-0.57	-1.60	(-2.0023 -2.0008 -0.5000)	75	-11.37
A1	-0.44	-1.68	(-1.9997 -1.9996 -0.5000)	92	-20.67
A2	-0.43	-1.59	(-2.0001 -2.0007 -0.5000)	78	-22.83
A3	-0.39	-1.51	(-2.0004 -2.0000 -0.5000)	76	-22.79
A4	-0.39	-1.59	(-2.0099 -2.0099 -0.5000)	100	-22.30
A5	-0.33	-1.60	(-2.0029 -2.0029 -0.5000)	74	-24.32
A6	-0.52	-1.66	(-2.0038 -2.0142 -0.5001)	77	-21.41
A7	-0.55	-1.78	(-1.9991 -2.0098 -0.4999)	76	-16.71
A8	-0.34	-1.61	(-2.0014 -2.0054 -0.5001)	84	-24.99

### 3.2.4 Marshal-Olkin Copula

Marshal-Olkin copula is from non-Archimedean copula family. It is used in image change detection algorithms [13] and here we are applying it to the area based image registration. Here the alignment measure is the negated mutual information. As can be seen in Table 3.4, the registration is not accurate as PSNR values are very small (far from zero). Also we can see in Final AM column, the values are -1.24 which indicates that  $\tau > 0.8$ , (section 2.3.3) where the mutual information decreases for Marshal Olkin copula and the optimization algorithm stops at this point. Hence the Marshal-Olkin copula was not successful in order to register the tested images.

Table 3.4: Image registration results for Marshal-Olkin Copula

Images	InitialAM	FinalAM	FinalT	Iterations	PSNR
P1	-1.03	-1.24	(-1.8183 -2.5884 -0.5063)	75	-17.79
P2	-1.07	-1.24	(-2.4841 -2.5740 -0.4954)	79	-18.01
P3	-1.05	-1.24	(-2.7930 -1.8269 -0.4972)	72	-20.48
P4	-1.05	-1.24	(-2.0579 -2.7539 -0.5016)	75	-18.82
P5	-1.06	-1.24	(-1.7279 -1.2338 -0.5031)	80	-18.08
P6	-1.06	-1.24	(-1.9167 -2.5406 -0.5008)	71	-15.56
P7	-1.08	-1.24	(-1.2947 -1.5164 -0.5056)	68	-17.66
P8	-1.06	-1.24	(-1.3496 -2.1672 -0.5052 )	81	-17.68
A1	-0.89	-1.24	(-1.4370 -0.2514 -0.4963)	65	-27.74
A2	-0.87	-1.24	(-1.1359 -1.4990 -0.4890 )	77	-25.90
A3	-0.82	-1.24	(-1.7766 -3.0360 -0.5053)	78	-21.50
A4	-0.89	-1.24	(-1.4370 -0.2514 -0.4963)	65	-25.62
A5	-0.73	-1.24	(-1.4682 -1.8742 -0.5149)	60	-25.13
A6	-0.99	-1.24	(2.7180 -1.4284 -0.4501)	54	-29.47
A7	-1.03	-1.24	(1.2575 1.6143 -0.4559)	73	-27.57
A8	-0.75	-1.24	(-2.9131 -2.2967 -0.5020)	73	-28.08

### 3.2.5 Gaussian Copula

Gaussian copula as defined in the previous chapter is one of the elliptical copula families and used to calculate the mutual information. Here the alignment measure is the negated mutual information. Table 3.5 presents the results of the Gaussian copula based image registrations for 16 images.

Table 3.5: Image registration results Gaussian Copula

Images	InitialAM	FinalAM	FinalT	Iterations	PSNR
P1	-0.38	-2.37	(-1.9979 -2.0003 -0.5001)	81	-12.76
P2	-0.51	-2.55	(-1.9992 -1.9983 -0.5000)	71	-12.84
P3	-0.47	-2.33	(-2.0015 -2.0021 -0.5000)	72	-12.70
P4	-0.48	-2.55	(-1.9989 -1.9996 -0.4999)	73	-12.14
P5	-0.51	-2.59	(-2.0012 -1.9996 -0.5000)	74	-11.05
P6	-0.72	-2.45	(-1.9973 -2.0037 -0.4999)	82	-11.41
P7	-0.52	-2.68	(-2.0020 -2.0012 -0.4999)	90	-10.52
P8	-0.54	-2.70	(-2.0001 -1.9987 -0.5000)	82	-11.37
A1	-0.15	-1.73	(-2.0058 -2.0015 -0.5000)	97	-20.67
A2	-0.08	-1.40	(-2.0043 -2.0046 -0.5000)	82	-22.83
A3	-0.17	-1.34	(-2.0110 -2.0044 -0.4999)	80	-22.79
A4	-0.12	-1.40	(-2.0078 -2.0156 -0.4999)	87	-22.30
A5	-0.07	-1.40	(-2.0065 -2.0069 -0.4999)	74	-24.32
A6	-0.10	-1.48	(-2.0148 -2.0092 -0.4999)	79	-21.41
A7	-0.21	-2.01	(-1.9816 -1.9816 -0.4997)	76	-16.70
A8	-0.09	-1.41	(-2.0025 -2.0066 -0.4999)	84	-24.99

In this method we obtained better result than the joint histogram method as the PSNR values are closer to zero. In Figure 3.4 the registration of the first aerial image (A1), using the Gaussian copula is presented. Here the Gaussian copula image registration base algorithm obtains the transformation as  $(-2.0058 -2.0015 -0.5000)$  in which the test image is translated  $-2.0058$  centimetres on the  $x$  axis and  $-2.0015$  centimetres on the  $y$  axis and rotated  $-0.5000$  radius. The obtained transformation is very close to the reference transformation values that is  $(-2, -2, -0.5)$ .

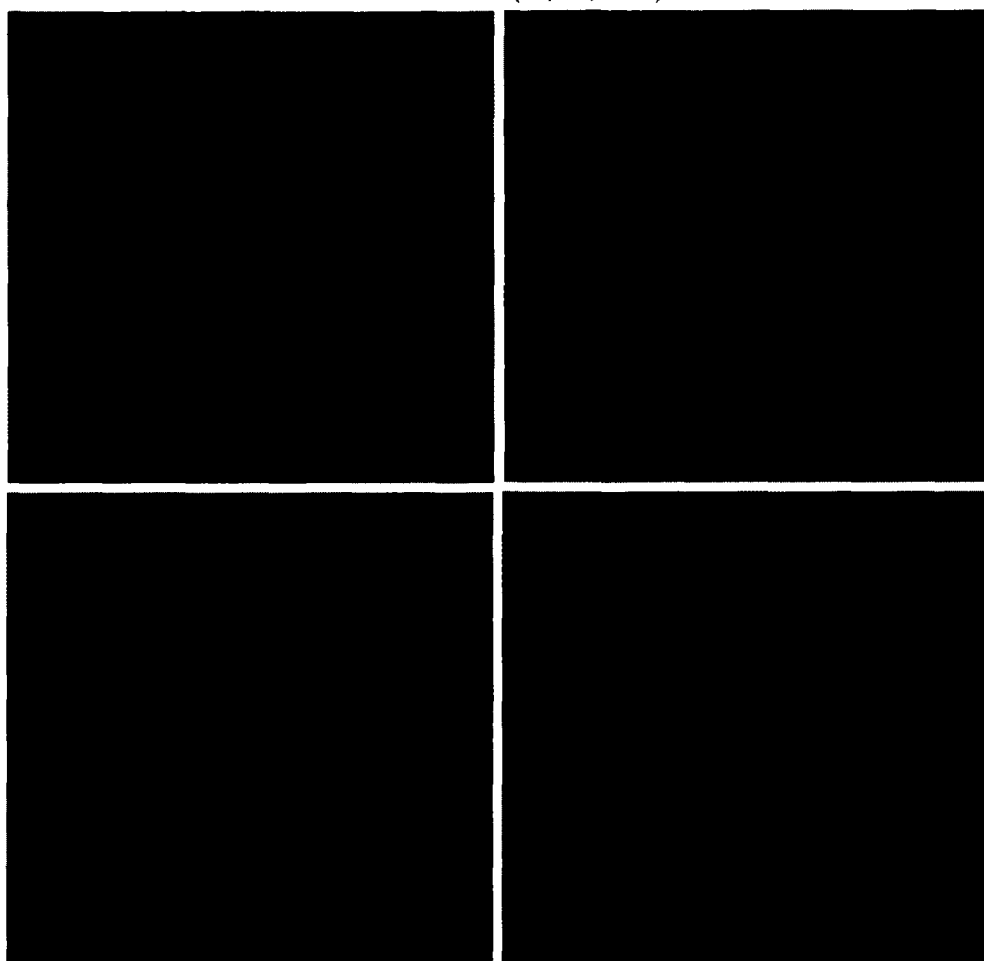


Figure 3.4: First aerial image which registered using the Gaussian copula method. (first row left: the reference image, first row right: the test image, second row left: the registered test image, second row right: the overlap of registered test image on the reference image)

### 3.3 Summary of Experiments

We may summarize the image registration results obtained in the previous section using Figures 3.5 and 3.6. In Figure 3.5, we can see the PSNR values of the eight registered MRI images. According to this figure the joint histogram, Gaussian and Frank copulas obtained similar results and Clayton copula and Marshal-Olkin were not successful copulas for the tested images. Figure 3.6, presents the PSNR results for the 8 aerial images. In this figure also we see the similar pattern as Figure 3.5. Figure 3.6, shows that the joint histogram method miss-registered the first aerial image. Also on these figures we can see that the Marshal-Olkin copula and Clayton copula resulting in miss-registered images in comparison with the other copula based methods. In Figure 3.6, we can see the Marshal-Olkin registration, have the best performance for third aerial image and worst performance for fifth aerial image.

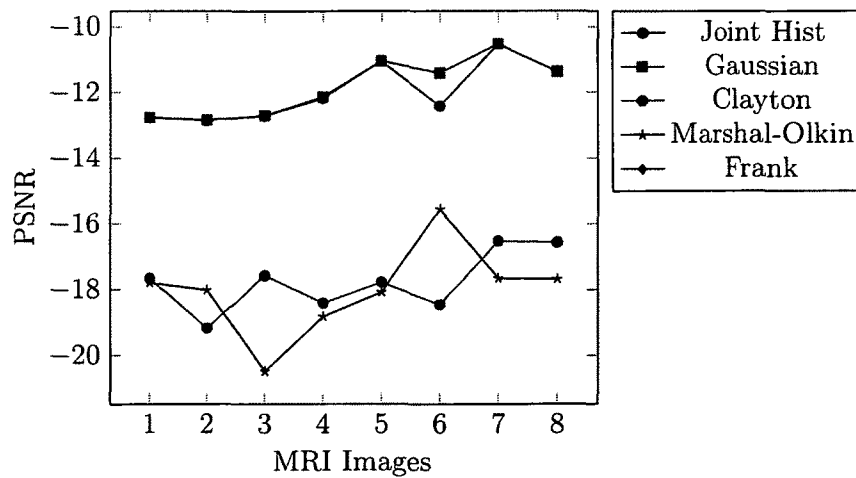


Figure 3.5: PSNR values for the 8 MRI images

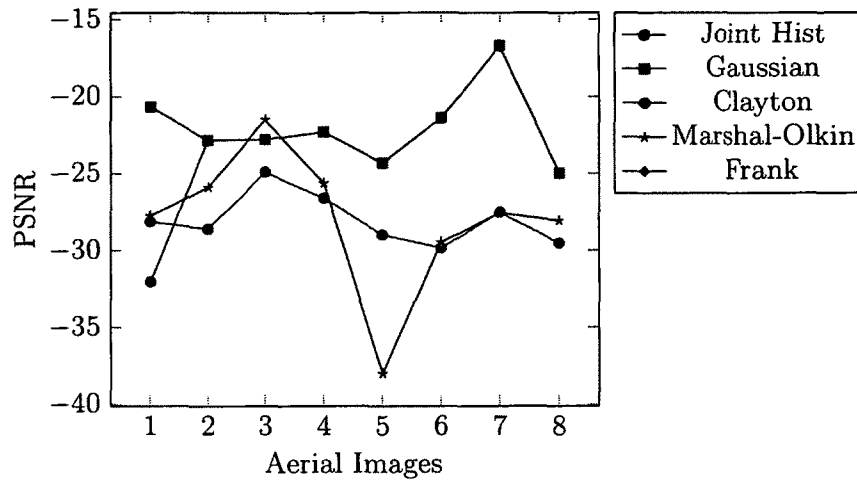


Figure 3.6: PSNR values for the 8 Aerial images

Another summary of the results in this thesis can be seen from the following figures. In Figure 3.7 and 3.8, we can see the path for optimization of the rotation radius, which starts from 0.2 radius rotation angle and reaches to the optimum rotation angle that is -0.5 radius. Figures 3.7 and 3.8, belong to the Gaussian copula registration of the fourth MRI and aerial images respectively. In these figures the rotation angle starts from the initial angle point that we provided to the `fminsearch` algorithm that is 0.2 radius and finally converges to a point close to -0.5 radius. The -0.5 radius rotation angle is the best possible rotation angle that can align the test image to the reference image. The `fminsearch` MATLAB optimization as described in [23], performs the initial simplex, contract outside, contract inside, expand and reflect stages in the number of iterations, until it reaches to the optimum point.

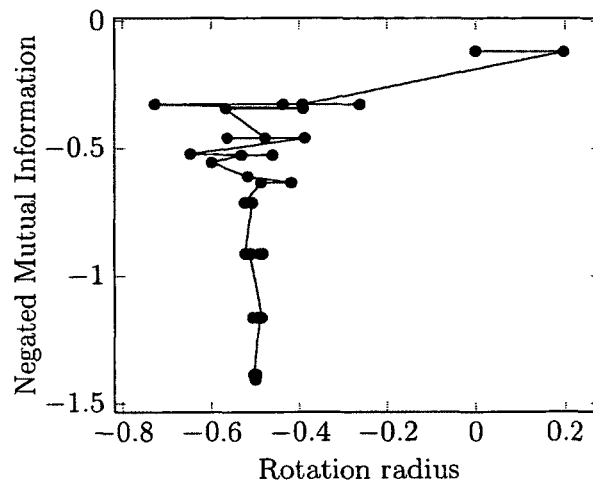


Figure 3.7: The optimization result of the Gaussian Copula for the 4th aerial image after 87 iterations

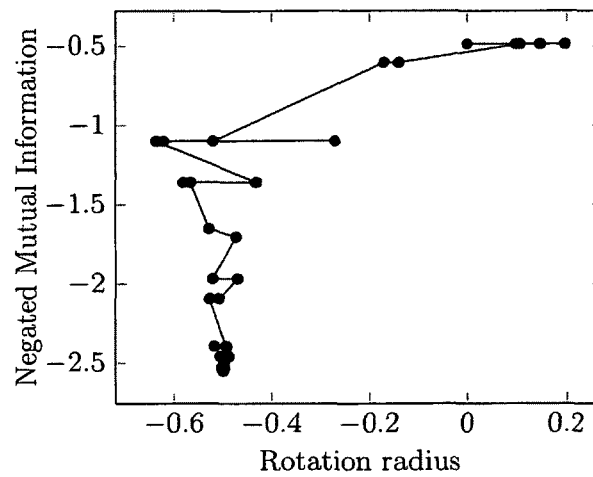


Figure 3.8: The optimization result of the Gaussian Copula for the 4th MRI image after 73 iterations

Figures 3.9 and 3.10, are the demonstration of the Gaussian copula based image registration of the fourth aerial and MRI images. We demonstrated the convergence of the rotation radius of these images in Figures 3.7 and 3.8. Here the Gaussian copula method obtain the transformation values as  $(-2.0078 -2.0156 -0.4999)$  and  $(-1.9989 -1.9996 -0.4999)$  for A4 and P4 images respectively. Note that in Figure 3.10 we can

see the reference and test MRI images along with the rectangular region of interest (ROI) of coordinates:  $[x_1=30, y_1=30, x_2=225, y_2=225]$ .

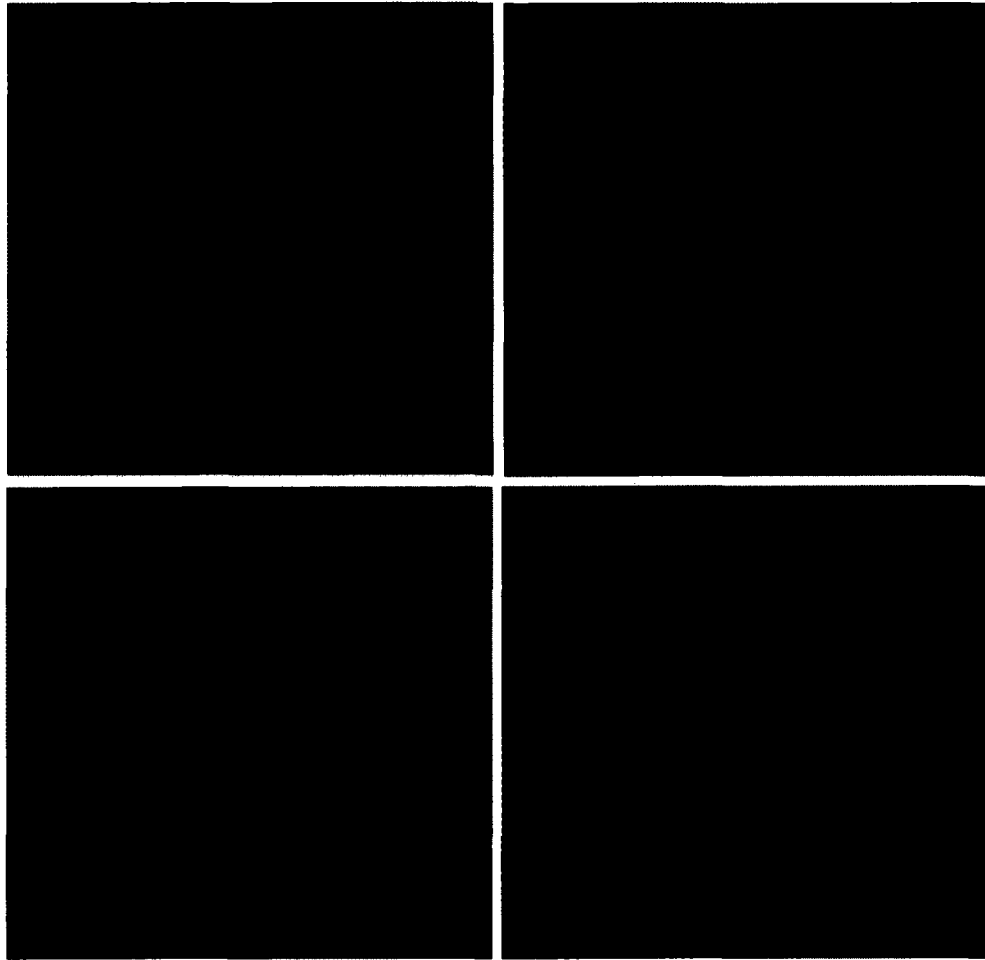


Figure 3.9: Registered image of the 4th aerial image.(first row left: the reference image, first row right: the test image, second row left: the registered test image, second row right: the overlap of registered test image on the reference image)

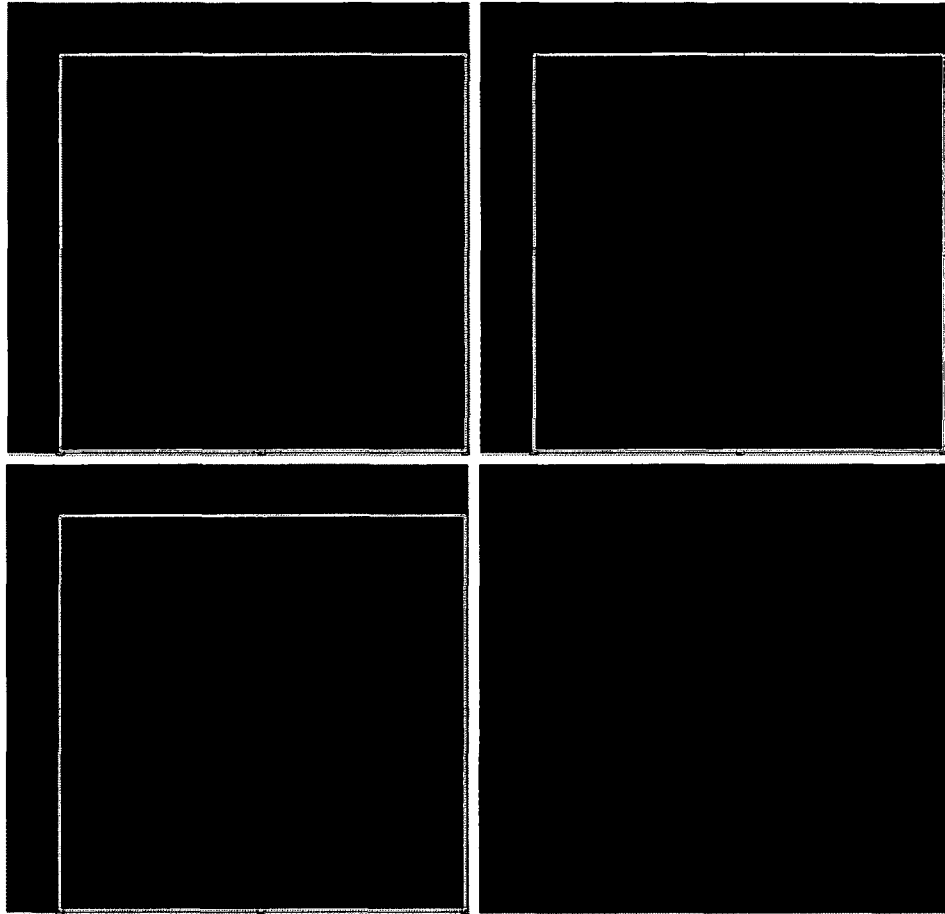


Figure 3.10: Registered image of the 4th MRI image.(first row left: the reference image with ROI, first row right: the test image with ROI, second row left: the registered test image with ROI, second row right: the overlap of registered test image on the reference image)

In image registration algorithms one important concern is the speed of the algorithms. The computer used in this research is an Intel Core i3 with 6 GB RAM on Windows 7 operating system. In this thesis the average speed of the performed algorithms are as follows:

Joint histogram: 29.494 seconds

Clayton:7663.788 seconds

Frank: 6025.555 seconds

Marshal:5995.018 seconds

Gaussian:7.900 seconds

The Gaussian copula performs faster than the other methods. The reason is that the major time consuming process of copula based algorithms are the Kendall's Tau calculation and Gaussian copula uses Pearson product correlation which is faster than Kendall's Tau. The reason for Kendall's tau's slow performance is the large size of the data. The data size in this thesis are  $256 \times 256 = 65536$  for each MRI image and  $188 \times 188 = 35344$  and  $177 \times 177 = 31329$  for each aerial image. Also aerial images take longer to process as they have more intensity value variations. Hence one of the future research topics can be the use of methods, in order to improve the speed of the Kendall's tau calculations.

## Chapter 4

# Summary and Concluding Remarks

Image registration is an ongoing area of research. There exists many crucial applications related to image registration and improvement of the image registration algorithm is an achievement.

In this thesis we tried to chose a particular algorithm of image registration. This particular algorithm consists of multi-view image, area-base algorithm, mutual information and divergence measure based alignment measure, rigid-body transformation and Downhill simplex optimization. We aim to monitor the performance of alignment measure. Here the performance of five alignment measures namely Clayton copula, Frank copula, Marshal-Olkin copula, Gaussian copula and joint histogram are monitored for the area based rigid body image registration. We only monitored the performance of the alignment metric function, where all other parameters were equal in experiments. For instance in the beginning of the research, to simulate the test images from the reference images we added random noise to the test images. The random noise may affect the equality of the experiments in order to compare the per-

formance of the alignment metric functions in image registration. Hence we did not add random noise and only performed geometrical translation and rotation on the reference images, in order to simulate the multi-view test images. The following are the main conclusions we could observe in this thesis:

1. We know that each copula family follows some constraints about the copula parameters used in the copula density functions, but for image registration we need to perform the experiments as we did in this thesis and see which copula function may suit the image registration algorithm. For the tested images and the particular image registration algorithm, the Gaussian and Frank copulas performed better than other tested copula functions.

2. The usage of copulas in image registration indeed is a new topic and this research may be continued in order to obtain faster and more accurate methods.

3. Slow algorithm was the main drawback of this research and in the core of it the Kendall's tau calculation, was time consuming due to the large size of the images. The slow operation of the Kendall's tau is mainly due to the large size of data. The size of MRI images used were  $256 \times 256 = 65536$  for each image and the size of aerial images used were  $188 \times 188 = 35344$  and  $177 \times 177 = 31329$  for each image. The Gaussian copula performed faster than other copulas, due to its usage of Pearson correlation instead of Kendall's Tau rank correlation. Hence applying methods, in order to make faster copula based image registration algorithm, might be a topic of future research.

4. As this is the beginning of the copula based image registration, these methods must be performed on the real life application such as 3 dimensional medical images and large aerial images.

Here a version of copula based divergence and mutual information based image registration algorithm was assembled in which four copula functions namely, Clayton, Frank, Marshal-Olkin and Gaussian copulas were used as alignment measures. These algorithms were tested on 16, two-dimensional gray-scale MRI and aerial images. In this combination the Frank and Gaussian copulas performed better than other copula functions. There are other copula functions that may be used in image registration algorithms. Also as we mentioned in chapter one, there are various image registration algorithms. Hence this research may be continued with other combinations of image registrations and other copula families in order to improve the speed and accuracy of the image registration outcome and they may be compared with the present thesis.

# Bibliography

- [1] R.B. Nelson, *An Introduction to Copulas*, Second edition, Springer, 2006.
- [2] B. Zitova, J. Flusser, Image registration methods: a survey, *Image and Vision Computing* 21, 9771000, 2003.
- [3] L.M.G. Fonseca, B.S. Manjunath, Registration techniques for multisensor remotely sensed imagery, *Photogrammetric Engineering and Remote Sensing* 62, 10491056, 1996.
- [4] B. Likar, F. Pernus, A hierarchical approach to elastic registration based on mutual information, *Image and Vision Computing* 19, 3344, 2001.
- [5] D.L.G. Hill, P.G. Batchelor, M. Holden, D.J. Hawkes, Medical image registration, *Physics in Medicine and Biology* 46, R1R45, 2001.
- [6] P. Kumar, Applications of the Farlie-Gumbel-Morgenstern Copulas in Predicting the Properties of the Titanium Welds, *International Journal of Mathematics*, 1, 1, 13-22, 2009.
- [7] P. Kumar, *Copula Functions as a Tool in Statistical Modelling and Simulation*, Proceedings of the International Conference on Methods and Models in Computer Science (ICM2CS09), IEEE Xplore, 2009.

- [8] A.W. Marshall, I. Olkin, Families of Multivariate Distributions, *Journal of the American Statistical Association*, 83, 834-841, 1988.
- [9] E.W. Frees, E. Valdez, Understanding Relationships Using Copulas, *North American Actuarial Journal*, 2, 1, 1-25, 1998.
- [10] J.P.W. Pluim, J.B.A. Maints, Antoine , M.A. Viergever, Mutual-Information-Based Registration of Medical Images: A Survey , *IEEE TRANSACTIONS ON MEDICAL IMAGING*, 22, 8, 2003.
- [11] R.C. Gonzalez, R.E. Woods, S.L. Eddins, Image processing using Matlab, *Pearson, India*, 2009
- [12] G. Mercier, S. Derrode, W. Pieczynski, J.M. Nicolas, A. Joannic-chardin, J. Inglada, Copula-based Stochastic Kernels for Abrupt Change Detection, *IEEE*, 2006 .
- [13] G. Mercier, G. Moser, S. Serpico, Conditional Copula for Change Detection on Heterogeneous Data, *GET / ENST Bretagne / dpt ITI CNRS UMR 2872 TAMCIC, Equipe TIME*, 2006.
- [14] T.S. Durrani and X. Zeng, Copula based Divergence Measures and their use in Image Registration, *17th European Signal Processing Conference EUSIPCO* , 2009.
- [15] F. Maes, A. Collignon, D. Vandermeulen, G. Marchal, P. Suetens, Multimodality image registration by maximization of mutual information, *IEEE Trans, Med Image*, vol 16, no.2, 187-198, 1997.
- [16] P. Viola, W.M. Wells, Alignment by Maximization of Mutual Information, *International Journal of Computer Vision* 24(2), 137-154, 1997.

- [17] X. Zeng and T.S. Durrani, Estimation of mutual information using copula density function, *ELECTRONICS LETTERS 14th* Vol. 47 No. 8, 2011.
- [18] A. Collignon, F. Maes, D. Delaere, D. Vandermeulen, P. Suetens, and G. Marchal, Automated multimodality image registration using information theory, in Information Processing in Medical Imaging (IPMI'95) (Y. Bizais, C. Barillot, and R. Di Paola, Eds.), pp. 263-274. Dordrecht: Kluwer, 1995.
- [19] J. V. Hajnal, D.L.G. Hill, and D.J. Hawkes, Eds., Medial Image Registration, The Biomedical Engineering Series, CRC Press, Boca Raton, FL, 2001, ISBN 0-8493-0064-9.
- [20] A. Sklar, Fonctions de repartition a  $n$  dimensional et leurs marges, *Publ. Inst. Stat. Univ. Paris*, 8, 229-231, 1959.
- [21] P. Heidelberger and P. Shahabuddin, *Efficient Monte Carlo methods for Value at Risk*, Working Paper, Columbia University, 2000.
- [22] W. Hoeffding, Masstabinvariance korrelationsmasse, *Schriften des Mathematischen Instituts fur Angewandte Mathematik der Universitat Berlin*, 5, 3, 179-233, 1998.
- [23] J.C. Lagarias, J.A. Reeds, M.H. Wright, P.E. Wright, Convergence Properties of the Nelder Mead Simplex in Low Dimensions, *SIAM J. OPTIM* Vol 9, No 1 , 112-147, 1998.
- [24] <http://www.satimagingcorp.com/gallery-quickbird.html>.
- [25] <http://www.vuse.vanderbilt.edu/image/registration>
- [26] William (Sandy) Wells. Course materials for HST.582J / 6.555J / 16.456J,

Biomedical Signal and Image Processing, Spring 2007. MIT OpenCourseWare  
(<http://ocw.mit.edu>), Massachusetts Institute of Technology.

# Appendix A

## Software Licence and Versions

### A.1 MATLAB

MATLAB Version 7.7.0471(R2008b) September 17, 2008

Licence Number: 257533.

### A.2 Maple

Maple 13.01 Wednesday, July 8, 2009

Product Build ID 413217

Single User Profile

Licensed to: University of Northern British Columbia

Serial Number: YVKYTN55WTAZNVUF

# Appendix B

## Description of Images in Experiments

### B.1 MRI

14th slice of patients 1 to 8 MRI images with gray scale intensity values and JPEG format and 256 x 256 resolution.

### B.2 Aerial

A1: Location: Ukraine, Acquisition date: 9-Oct-2002, Sensor: Quick Bird

A2: Location: Greece, Acquisition date: 12-May-2004, Sensor: Quick Bird

A3: Location: Peru, Acquisition date: 9-Jan-2005, Sensor: Quick Bird

A4: Location: Guam, Acquisition date: 9-July-2002, Sensor: Quick Bird

A5: Location: Iran, Acquisition date: 26-June-2009, Sensor: Quick Bird

A6: Location: Russia, Acquisition date: 9-June-2004, Sensor: Quick Bird

A7: Location: Bahamas, Acquisition date: 27-Dec-2003, Sensor: Quick Bird

A8: Location: Saudi Arabia, Acquisition date: 30-Dec-2005, Sensor: Quick Bird

These aerial images are with gray scale intensity values and JPEG format. A1,A2,A3,A4,A5,A6 and A8 are with 188 x 188 resolution and A6 is with 177 x 177 resolution.